Relative permeabilities for two-phase flow through wellbore cement fractures

Anwar, Ishtiaque
Reda Taha, Mahmoud M.
Stormont, John C.
Hatambeigi, Mahya
Hart, David
Lord, David

To be published in: Geoenergy Science and Engineering

DOI to publisher's version: 10.1016/j.geoen.2024.213111

Journal Pre-proof

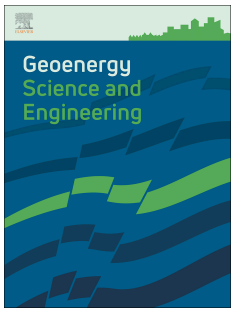

Relative permeabilities for two-phase flow through wellbore cement fractures

Ishtiaque Anwar, Mahya Hatambeigi, Mahmoud Reda Taha, David B. Hart, David L. Lord, Meng Meng, John C. Stormont

PII: S2949-8910(24)00481-0

DOI: https://doi.org/10.1016/j.geoen.2024.213111

Reference: GEOEN 213111

To appear in: *Geoenergy Science and Engineering*

Received Date: 8 April 2024

Revised Date: 20 June 2024

Accepted Date: 6 July 2024

Please cite this article as: Anwar, I., Hatambeigi, M., Taha, M.R., Hart, D.B., Lord, D.L., Meng, M., Stormont, J.C., Relative permeabilities for two-phase flow through wellbore cement fractures, *Geoenergy Science and Engineering*, https://doi.org/10.1016/j.geoen.2024.213111.

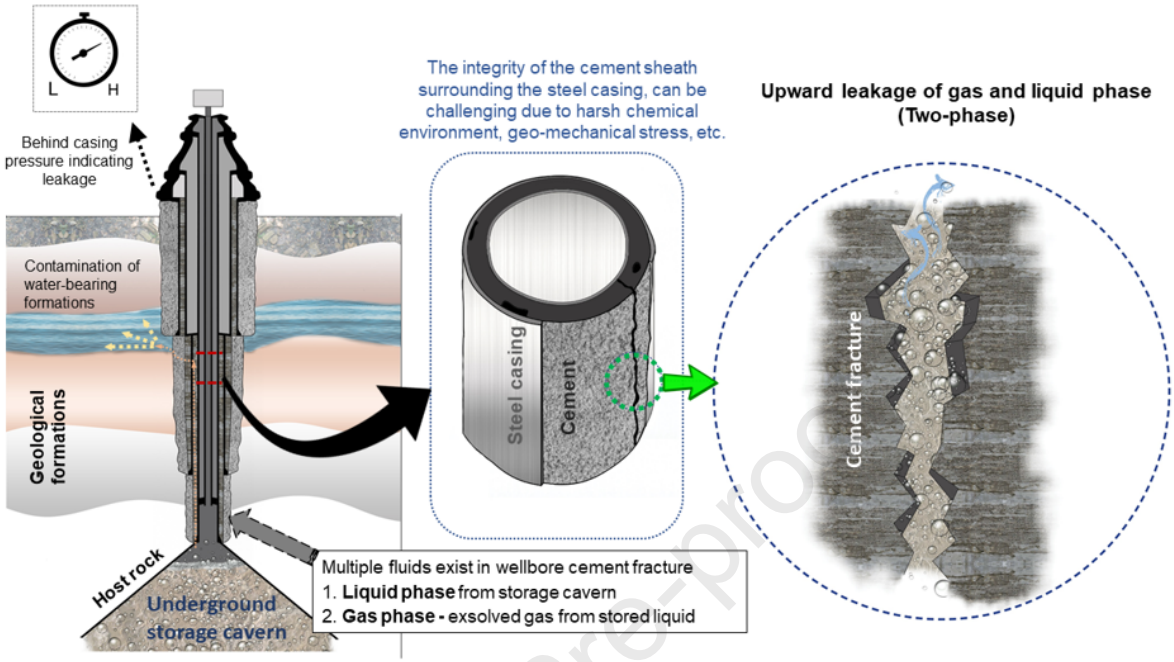

Relative permeabilities for two-phase flow through wellbore cement fractures

Ishtiaque Anwar[1,3], Mahya Hatambeigi[1], Mahmoud Reda Taha[1],
David B. Hart[2], David L. Lord[2], Meng Meng[3], and John C. Stormont[1].

[1] University of New Mexico, Albuquerque, NM, United States

[2] Sandia National Laboratories, Albuquerque, NM, United States

[3]Los Alamos National Laboratories, Los Alamos, NM, United States

Abstract

Multiple fluids are likely to exist in fractures and flow paths associated with leaky wellbores, including liquids (e.g., crude oil) and gases (e.g., gas exsolved from liquid). These fluids occupy and move through different portions of the pore spaces within the fractures depending on many factors, including fluid properties, fracture size, and the amount of the different fluids. Upward leakage of any phase, through the fracture, can contaminate water-bearing formations, create hazardous surface conditions, and compromise the functionality of the wellbore. Early signs of wellbore leaks may be expressed by anomalous pressure behavior at surface monitoring points on cavern storage wells. These pressure anomalies are difficult to interpret, necessitating knowledge of the factors that affect the multiphase flow in fractures and porous media. These parameters are critical to modeling multiphase flow in fractures. This insight can guide further diagnosis and maximize leak remediation. Our study focuses on the relationship of the liquid–gas relative permeabilities for representative variable-aperture wellbore cement fracture. To obtain the relative permeability of each phase, two-phase flow tests were conducted where both fluids were flowing simultaneously through a fractured wellbore cement specimen under a range of factors, namely (1) aperture size, (2) capillary numbers, and (3) viscosity ratio. The flow experiments were conducted under a range of confining stresses and flow velocities, using nitrogen gas and silicone oils (of different viscosities) in a specially designed pressure vessel. The sum of gas and oil relative permeabilities were found to be less than one under all conditions, which indicates that the presence of one phase affects the permeability of the other phase, and vice versa. Since the gas phase flow conditions include a significant inertial flow component in addition to viscous flow, the inertial flow coefficients at different saturation states are presented. The factors affecting the relationship between the relative permeabilities are discussed in detail. A new mathematical model for estimating the relative permeability of wellbore cement fracture is presented and experimentally validated.

Keywords: leaky wellbore; two-phase flow; relative permeability; wellbore cement; rough fractures;

1. Introduction

Wellbores are used to provide subsurface access for a wide extent of operations, including fluid storage (Miyazaki, 2009), CO_2 sequestration (Theresa Lucy Watson & Bachu, 2008; M. Zhang & Bachu, 2011), geothermal energy development (Shadravan, Ghasemi, & Alfi, 2015), waste disposal, and oil/gas exploration and production (Davies et al., 2014). Wellbores are also used to extract natural gas from hydrate reservoirs in the ocean (Shaibu, Sambo, Guo, & Dudun, 2021). Multiple fluids are likely to exist in wellbore flaws depending on the facility the wellbore is associated with. Crude oil, such as that commonly stored in the Strategic Petroleum Reserve (SPR) caverns, can exhibit complex physical and chemical alterations due to pressure and temperature variation as it contains a variety of hydrocarbons ranging from dry natural gas to tar (Mullins, 2008; Toner, 1987). A significant amount of dissolved gases can evolve as a separate fluid phase (gas) from crude oil with the variation in pressure (Joshi, Mullins, Jamaluddin, Creek, & McFadden, 2001; McCain Jr, 2017; Mullins, 2008) and can leak simultaneously. The storage of CO_2 in deep geological formations entails several processes such as phase transition, CO_2 dissolution, and mineral precipitation, and other chemical reactions (Berkowitz, 2002; Ren, Ma, Wang, Fan, & Zhu, 2017), resulting in two-phase leakage at CO_2 sequestration wells and CO_2 driven enhanced oil recovery (EOR) sites. Similarly, two-phase fluid flow is possible in geothermal reservoirs. The presence of various, closely interrelated effects such as heat exchange with the geological formation, pressure variation in the stored fluid, and heat and mass transfer between the phases due to evaporation and desorption can cause a two-phase mixture of geothermal fluids ascending up the well (Barelli, Corsi, Del Pizzo, & Scali, 1982; Gould, 1974). The underground storage of radioactive nuclear wastes can also generate multiple gases, depending on the type of disposed waste. Studies indicate that the pressure of the exsolved gas from the stored radioactive waste is significant (Ortiz, Volckaert, & Mallants, 2002; Postgate, 1979; Reardon, 1995), making the flow of multiple fluids possible through the flow paths associated with leaky wellbores.

Advective two-phase leakage (flow of gas and liquid) through a wellbore flaw is likely. The build-up of fluid pressure in the cemented annulus at the surface, referred to as sustained casing pressure, is a far-reaching concern of numerous gas and oil wells (Davies et al., 2014; M. Zhang & Bachu, 2011). Hydrocarbon leakage, water and soil contamination,

and air pollution are all potential environmental consequences of SCP. In terms of operations, SCP has the potential to compromise well integrity, leading to possible blowouts - a dangerous occurrence that can endanger both humans and facility. Upward leakage of any individual phase, through wellbore flaws, can contaminate water-bearing formations, create hazardous surface conditions, and finally, compromise the functionality of the wellbore. A leaking wellbore may lead to the accumulation of hazardous or toxic fluid in the vicinity of the wellbore system. It is important to be able to estimate the potential leakage of any individual phase in order to assess the performance and safety of a wellbore. Early signs of wellbore leaks may be expressed by anomalous pressure behavior at surface monitoring points on cavern storage wells, especially in annual spaces that should be isolated from product pressures. Interpreting these pressure anomalies is complicated, requiring an understanding of the multiple factors that affect pressure and multiphase flow in fractures and porous media. Nemer et al. (2016) provided examples of the deviation of the wellhead pressure response during well integrity tests from single phase behavior, and suggest the need for two-phase flow to be considered. Qiao et al. (2023) describe limitations in single-phase models in capturing the behavior that leads to sustained casing pressure. The current work attempts to characterize the relationship between relative permeabilities of oil and gas in cement fracture environments relevant to leaky wellbore systems. These parameters are critical to modeling multiphase flow in fractures, which can improve understanding of how what is observed at the surface is related to potential leak behavior downhole. This knowledge can help direct additional diagnostics and ultimately optimize remediation of the leaks.

Potential leakage pathways have been identified in the wellbore system (Anwar, Carey, Johnson, & Donahue, 2022), including cement fractures, microannuli from de-bonding at the cement-casing and cement-formation interface (Celia, Bachu, Nordbotten, Gasda, & Dahle, 2005; Theresa L Watson & Bachu, 2009), and the porous corrosion product that may exist in between cement and steel casing (Anwar, Chojnicki, Bettin, Taha, & Stormont, 2019). The current study discusses the two-phase flow through the comparatively tortuous and complex variable aperture cement fractures. A simplified schematic of two-phase leakage in a leaky wellbore through a cement fracture is illustrated in Figure 1.1

The physics of two-phase flow (gas and liquid) through wellbore fracture is much more complicated than flow through unconfined smooth parallel plates made from homogenous materials, as it involves the effects of flow geometry, variation in wettability, external forces, etc. (Holtzman, 2016; Holtzman & Juanes, 2010; Holtzman & Segre, 2015; Or, 2008). The immiscible two-phase fluid movement through the thin gap between parallel plates is a classical problem and has been the focus of various scientific studies for porous and fractured media over the past few decades (Lenormand, Zarcone, & Sarr, 1983; Saffman & Taylor, 1958). However, characterization of the immiscible fluid flow remains a challenging issue in part due to the variable aperture size void spaces causing complex interaction between the capillary pressure from the fluid-fluid interface at the local scale and the nonlocal viscous pressure (He, Kahanda, & Wong, 1992).

The details of the movement of immiscible fluids (gas and liquid) through fractured media depend on the network of void spaces. The pore size distribution and tortuosity of the fracture depend on the external confining stress as the fracture is deformable. Previous studies on multiphase flow through fractures mostly focused on flow structure and permeability or on the fluid occupancy and invasion morphology of one phase displacing another (T Babadagli, Raza, Ren, & Develi, 2015; Tayfun Babadagli, Ren, & Develi, 2015; Karpyn, Grader, & Halleck, 2007; P. G. Persoff, Pruess, & Myer, 1991; Reitsma & Kueper, 1994). These studies indicate that the competition between capillary and viscous forces exert a significant influence on the dynamics of two-phase fluid through the fracture (Anwar, Carey, Johnson, & Donahue, 2021; Anwar, Hatambeigi, Chojnicki, Reda Taha, & Stormont, 2020), which is further complicated by the flow geometry of the variable aperture fracture (Nicholl & Glass, 2005), which can vary due to applied stress.

Lenormand et al. (Lenormand et al., 1983) used a simplified phase diagram with an attempt to show the effect of the capillary and viscous forces on two-phase flow. They employed two key dimensionless parameters, capillary number, and viscosity ratio. Capillary number (Ca) for flow through a fracture is a dimensionless ratio of viscous forces to capillary forces for a two-phase flow. The viscosity ratio (M) is defined as the ratio of the kinematic viscosity of the two fluid phases. However, all these investigations were restricted to porous media.

Although the fluid dynamics controlling two-phase flow in fractures is the same as in porous media, there are significant differences in the flow path geometry as well as tortuosity (Nicholl & Glass, 2005). The roughness of the wellbore cement fracture surfaces produces variable void sizes. The size difference among the void spaces for the two-phase flow can alter the balance between the capillary and viscous forces that govern the flow of both phases. However, in another study of two-phase flow displacement, visualization techniques are applied to observe the influence of viscous/ capillary forces on the dynamics of the fluid displacement process in a rough fracture (Y.-F. Chen, Wu, Fang, & Hu, 2018). Both studies relied solely on liquid displacement and did not include any confining stress on the fracture.

The purpose of the current study is to evaluate the major factors affecting two-phase flow through wellbore cement fracture from the experimental data and to compare the findings with the commonly used conceptual models used for estimating relative permeabilities. This study will be able to lead to more accurate predictions of the leakage rates of both wetting and non-wetting phases in a leaky wellbore.

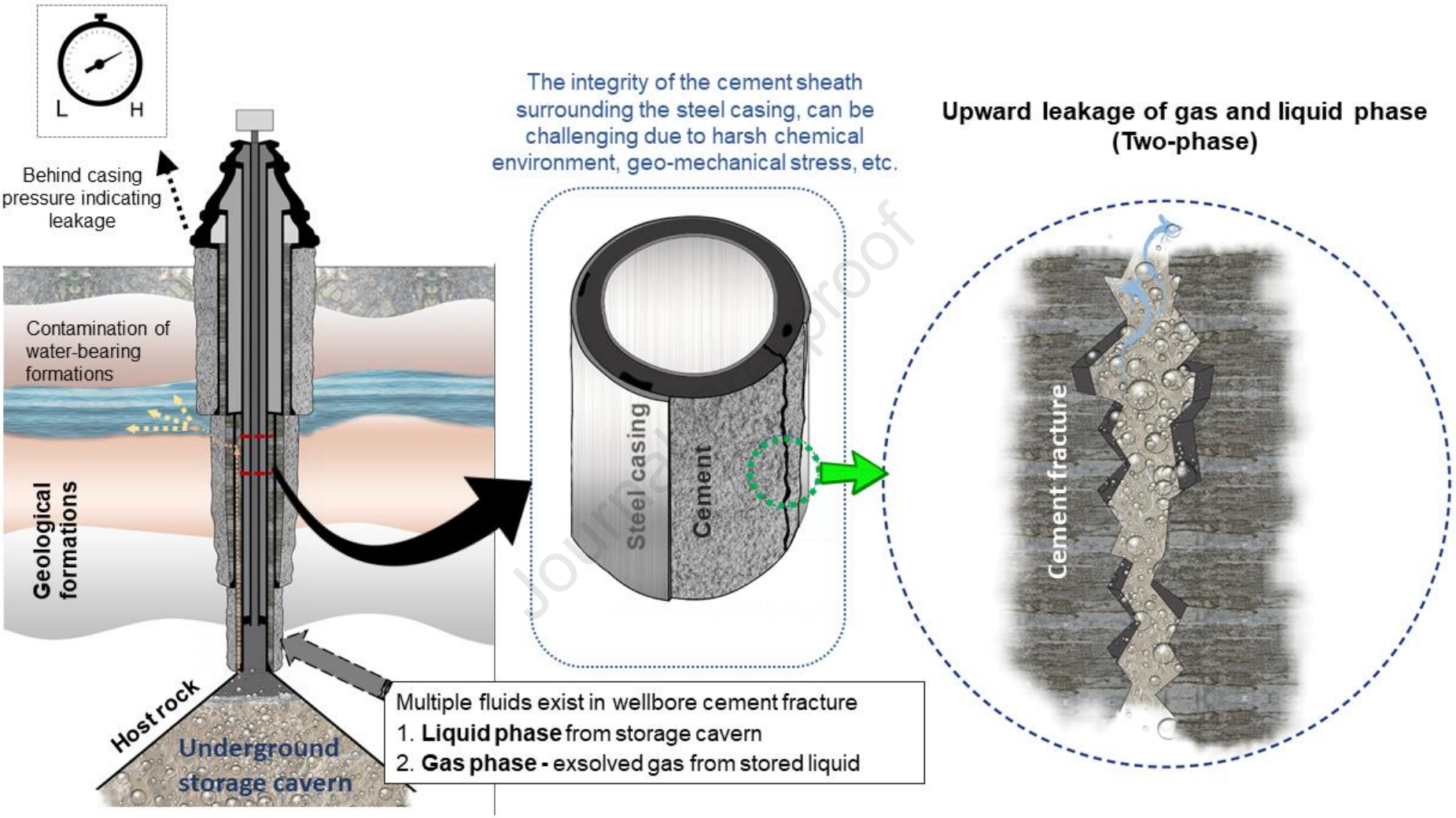

Figure 1.1 - Simplified schematic of two-phase leakage in a leaky wellbore through a variable aperture cement fracture

Existing conceptual models: A limited number of widely used conceptual relative permeability models, are discussed here, with features and limitations of each. The effective permeability of an individual phase is expressed as a dimensionless number referred to as the relative permeability, which is the ratio of the effective permeability of the phase to its saturated single-phase permeability.

Porous media approach: One commonly used approach to model two-phase flow is referred to as the porous medium approach. In this case, the cement fracture would be represented as a connected porous media. Such models assume that the pore space occupied by an individual phase is not available to the other phase. A large number of permeability models for the porous media exist in the literature that describes the relationship between the relative permeabilities in a two-phase flow system are mainly of two types: empirical models and geometric models. Empirical models are based on the data fitting of previous experimental data (Corey, 1954; Pirson, 1958), whereas, in geometric models, mathematical expressions of relative permeabilities are derived from retention curves or capillary pressure–saturation relationship (Brooks & Corey, 1964; Farrell & Larson, 1972; Gardner, 1958; Van Genuchten, 1980). The most commonly used relationships for relative permeabilities in porous media are power laws (Corey, 1954), such as Corey's model (Equation 1) (Corey, 1954), which is widely used by petroleum engineers.

$$Kr_g = \left(1 - \sqrt[4]{Kr_l}\right)^2 \left(1 - \sqrt[2]{Kr_l}\right) \quad (1)$$

Where *Kr* is the relative permeability of fluids, and the subscripts *g* and *l* refer to gas (non-wetting fluid) and liquid (wetting fluid), respectively.

Investigation on two-phase flow (air-water) using clay bricks, smooth glass plates, and artificially roughened glass plates was undertaken by researchers (Fourar & Bories, 1995; Fourar, Bories, Lenormand, & Persoff, 1993; Fourar, Piquemal, & Bories, 1991). They observed differences in flow structure (bubbles, slugs, channels, etc.) as well as strong phase interference at intermediate saturation. Experimental studies of two-phase flow through a transparent replica of rock fracture also displayed a strong phase interference (P. G. Persoff & Pruess, 1993; P. G. Persoff et al., 1991; P. Persoff & Pruess, 1995). The

studies characterized the flow of an individual phase possessing a localized continuous path that undergoes blocking and unblocking by the other phase. Multiple parameters, such as fluid characteristics, fracture size, and the quantity of various fluids, affect two-phase flow through various regions of the pore spaces within the fractures. Therefore, the aforementioned investigations ought to take into account the impact of confining stress on fracture or the capillary number/viscosity ratio of fluid phases.

The porous media approach is evaluated for two-phase flow through porous materials. As mentioned earlier, the flow path geometry of a porous medium and variable aperture fracture can be substantially different. As such, the two-phase flow mechanism through rough wellbore cement fracture may not always act as a porous medium.

Viscous coupling model (Pipe flow approach): Two-phase flow can be modeled using an approach similar to that for two-phase flow through a pipe, where it is assumed that the diameter is large enough to accommodate two fluid phases, dissimilar to capillary flow. For pores with a relatively larger diameter, both fluid phases simultaneously flow through the network by balancing the viscosity by the fluid inertia, body forces, and pressure gradient (Kundu, Cohen, & Dowling, 2008) with strong interaction or viscous coupling between the phases (De Gennes, 1983; Kalaydjian & Legait, 1987). Due to the interaction or coupling between the fluid phases with different viscosities flowing simultaneously, it is often called the viscous coupling model for two-phase flow. The fluid interactions during two-phase flow are observed in several experimental observations (Fourar et al., 1993, 1991; Kouame, 1989). A simplified expression of the viscous coupling model is presented in Equation 2.

$$Kr_l = \frac{1}{2}\left(1 - \sqrt[3]{Kr_g}\right)^2 \left(2 + \sqrt[3]{Kr_g}\right) \qquad 2$$

A study on oil-water displacement in a natural limestone fracture concluded that the capillary pressure curves could be well represented by a Brooks-Corey porous-medium-type capillary pressure function (Reitsma & Kueper, 1994). One study suggested that the flow through a single fracture can be simplified by treating it as a limiting case of porous media flow and by using a relative permeability approach (Diomampo, 2001). The effect of channeling in two-phase flow through artificial and uniform rough fractures due to the

variation in flow configuration was investigated by researchers (C. Chen & Horne, 2006; Wong, Pan, & Maini, 2008). More recently, studies on transparent replicas of real rough fractures (rock) were used to evaluate multiphase flow characteristics within the non-Darcian regime, including relative permeabilities (Nowamooz, Radilla, & Fourar, 2009; Radilla, Nowamooz, & Fourar, 2013) for relatively large fractures (minimum fracture aperture > 0.4 mm) instead of a real rock or cement fracture. These studies also assumed that the relative permeabilities solely depend on the phase saturation. Two-phase flow through different portions of the pore spaces within the fractures depends on multiple factors, including fluid properties, fracture size, and the amount of the different fluids. Therefore, the effect of confining stress on fracture or capillary number/ viscosity ratio of fluid phases should be included in the above-mentioned studies.

The complex pore network of wellbore cement fracture contains both smaller and larger pores, and it varies with different factors such as fracture surface roughness, geostatic stress, etc. As such, the viscous coupling model, which does not include the capillary flow that occurs for relatively smaller pores, may not be adequate to define the two-phase leakage in a leaky wellbore completely. In other words, the variation in pore sizes along the flow network of rough cement fracture can alter the balance between the capillary flow and viscous coupling flow, making the model less effective in defining the relationship between relative permeabilities.

X – curve, a simplified model: Two-phase flow through relatively large smooth walled fracture may create parallel flow channels of almost equal flow rate, which can be described using X – curve or X – model (Maloney & Doggett, 1997; Romm, 1966). For X - curve, it is assumed that the sum of relative permeabilities is equal to one, indicating the absence of phase interference during the flow, displaying a linear relationship between the relative permeability and phase saturation (Maloney & Doggett, 1997; Romm, 1966). The X - curve is often used by engineers for its simplicity. Mathematically it can be expressed as

$$Kr_l = 1 - Kr_g \qquad 3$$

Liquid-liquid two-phase flow through a smooth-walled artificial fracture with a relatively large aperture (> 2mm) was investigated in the past, which was used to develop the X-

model for the relationship between relative permeabilities (Romm, 1966). It has been observed that the sum of relative permeabilities equals one, as described by the X – model, which are not appropriate for many applications (Fourar et al., 1991; Pruess & Tsang, 1990).

Numerical simulations can describe two-phase flow in a single fracture with some success, but there are shortcomings such as accuracy, processing time, etc. Although several efforts to understand the two-phase flow behavior have been made using numerical solutions, the experimental investigations on two-phase flow through variable aperture fractures are limited due to the difficulties in specimen preparation and flow parameter measurements. Most of the existing experimental studies have used either relatively small specimens (fracture surface area < 5 cm x 5 cm) or artificial fractures of larger fracture size (about 1 mm) due to technical limitations. The previously mentioned models often beg the question of which one to use for two-phase flow in leaky wellbores. Although a few comparative studies (Ansari, Sylvester, Shoham, & Brill, 1990; Gomez, Shoham, Schmidt, Chokshi, & Northug, 2000; Kaya, Sarica, & Brill, 2001) attempt to answer this question for wellbore flow, the reliability of the obtained experimental data has left this issue unsettled. Detailed experimental studies on the two-phase flow through wellbore cement fracture are essential for evaluating a more accurate mathematical model (D A Reynolds & Kueper, 2002; David A Reynolds & Kueper, 2001) for wellbore fractures. The need for a more appropriate and simplified model or approach to estimate the relative permeability of any individual phase in the leaky wellbore through wellbore cement fracture has received little attention.

To our knowledge, none of the previous research has been exclusively focused on investigating the factors affecting the two-phase flow through the variable aperture cement fractures under confining stress that are common in leaky wellbores. All of the above-mentioned factors are common in any wellbore system, and a leaky wellbore will inevitably be exposed to these influences. Thus, understanding how these factors affect the leakage of two immiscible fluid phases is crucial. The models mentioned above are only valid for the capillary and viscous regimes and not capable of accounting for the inertial flow regime, which is possible in the leaky wellbores. As a result, none of the

model's estimations are adequate to explain the two-phase flow through rough wellbore cement fracture.

To summarize, all the abovementioned models or approaches can reasonably estimate two-phase flow given: (i) appropriate conditions and parameters stipulated by the model and (ii) certain flow geometry (pore size, aperture distribution, fluid type, etc.) that were defined by researchers. However, due to inadequate relevant experimental data, obtaining the necessary parameters and the selection of the most appropriate model to describe two-phase flow through a variable aperture fracture, likely to exist in leaky wellbores, remains an issue. The goal of our study is to contribute to the resolution of the above-mentioned issues.

The primary objective of the study is to obtain gas-liquid relative permeabilities from simultaneous gas-liquid two-phase flow tests on fractured wellbore cement specimens for different factors, namely (1) aperture size, (2) capillary numbers, and (3) viscosity ratio. Gas slip and inertial flow are important considerations that must be taken into account for the experimental measurements. These phenomena have been shown to have significant effects on two-phase flow through cement fractures. The flow experiments are conducted under a range of confining stresses and flow velocities using two immiscible and chemically inert fluids – nitrogen gas (as gas-phase) and silicone oils (as liquid-phase) of different viscosities in a specially designed pressure vessel. Silicone oil has a viscosity that is comparable to that of certain crude oil. The flow velocities of fluid phases and flow measurement data are reduced to interpret the permeability. As the gas phase flow conditions include inertial flow components in addition to viscous force, the inertial flow coefficients at different saturation states are evaluated. The obtained results from the experimental study are compared with some commonly used relative permeability relationships (X – curve, porous media approach, and viscous coupling model). Additionally, we have introduced a new model for estimating the relative permeability of cement fractures.

2. Material and methods

Specimen preparation: The specimens for two-phase flow test were prepared from oil well cement, also known as wellbore cement. The mixture consisted of API Class G

Portland cement, silica fume (BASF Rheomac SF100), plasticizer (BASF Glenium 3030), and distilled water. The paste was mixed until a smooth and homogenous slurry was achieved with a water-cement ratio of 0.4. The mix design is in accordance with ASTM C305. The cement mixes were cured in a 55˚C (131 °F) water bath for seven days and were stored until tested in a 100% humidity curing room.

The hardened class G cement cylinders were prepared in the laboratory with a nominal cured dimension of 152 mm (5.98 in) in length and the outer diameter of 75 mm (2.95 in). A single fracture was introduced by tensile splitting (Fairhurst, 1964), which divides the cement cylinders longitudinally into two halves.

Flow test: The laboratory simultaneous two-phase steady-state flow test in a modified pressure vessel provides the relative permeabilities of each phase from direct measurements of flow and pressure gradients. The fluid flow tests were carried out by placing fractured cement specimens in a pressure vessel and subjected to a constant hydrostatic confining stress while measuring gas and liquid (oil) flow through the samples. A schematic of the experimental setup and a simplified diagram of the fracture sample subjected to stresses is shown in Figure 2.1. Hydraulically actuated end caps of the pressure vessel apply an equal axial stress to the specimen. The hydrostatic confining stress is monitored by a pressure gauge that had an accuracy of 0.01 MPa (1.45 psig). The fluid (gas or oil) pressure was applied to one side of the core holder containing the specimen, creating a pressure gradient across the specimen that results in flow from the higher pressure to the lower pressure. Using a pressure gauge, the downstream pressure was measured before being released into the atmosphere. The applied fluid pressure in the fracture is referred to as the pore pressure. The flow tests were conducted at 25 ± 0.5˚C (77 ± 0.9°F) under a range of confining stresses (3.45 MPa to 13.8 MPa), which corresponds to the expected geostatic stress at a depth of about 175 m to 700 m (574 ft to 2297 ft).

The experimental system is capable of measuring gas or liquid flow, which are largely two different experimental systems. Two separate lines for gas and liquid phases connect to an upstream endcap of the pressure vessel, where they mix before entering the cement fracture, flow through the sample, and exit via the downstream endcap into a separation

flask, where they are separated, and their flow rates are measured. The fluid pressures at both sides of the specimens were recorded continuously during the test using transducers that are connected to a computer via a signal conversion system.

Digital mass flow controllers (Alicat Scientific Inc.), calibrated for nitrogen gas, were used to measure, and control the gas flow rate during the test. Once the fluid flow rate is specified in the mass flow controller connected to the specimen's upstream side, the instrument automatically adjusts the valve to achieve the required flow during the two-phase flow test. The device also helps to achieve a steady-state condition relatively faster.

Depending on the flow rate, either a high-performance liquid chromatography (HPLC) grade pump (from Scientific Systems, Inc.) with self-flashing pump head, or a syringe pump (from Teledyne ISCO) is used for controlling the flow rate of wetting phase fluid (silicone oil). The system can deliver pulseless flow, and the flow rate is constant even with variable backpressure. The flow rate of the HPLC pump can be set in 0.01 ml increments from 0.01 to 10.00 ml/min with a precision of 0.5%. The flow rate of the syringe pump can be set in 0.1 ml increments from 1.00 to 400.00 ml/min with a precision of 0.1%.

At the beginning of each experiment, the specimen was saturated with pertinent silicone oil (wetting phase fluid) and single-phase oil flow tests were undertaken to determine the intrinsic permeability of each fracture. The oil flow tests were conducted at different flow rates and, consequently, slightly different pore pressures. Outflow collected during each test confirmed a steady flow for each test.

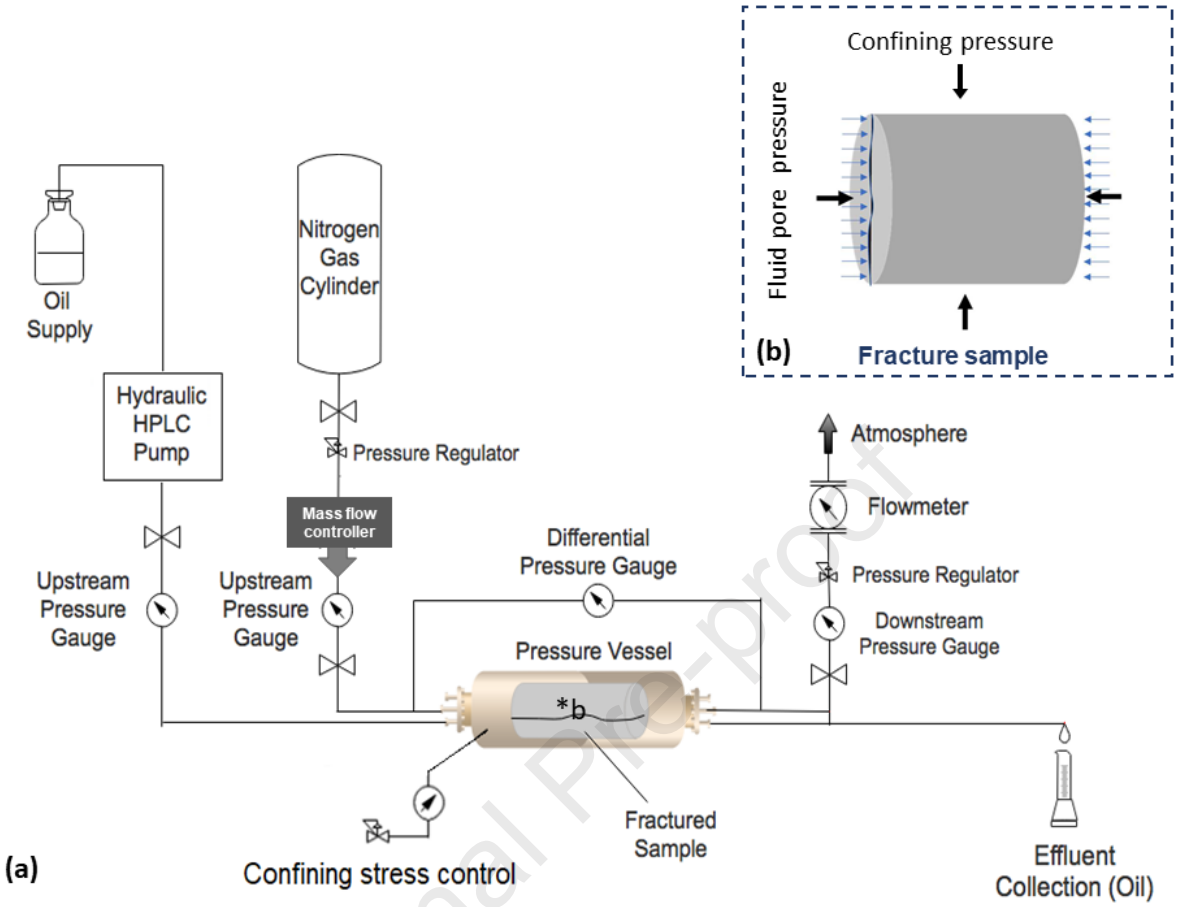

Figure 2.1 – (a) Schematic for the two-phase flow test configuration, (b) schematic of confining stress and fluid pressures applied to samples during testing.

Simultaneous two-phase flow

To assess the relative permeability of each fluid phase, flow experiments were undertaken in which both fluids were concurrently flowed through the fractured wellbore cement specimen. For the measurement, the fractured cement specimens were first saturated with wetting fluid (silicone oil), and a very low gas flow rate was introduced to one side of the specimens. The gas flow rate was then slowly increased, maintaining a constant upstream oil flow rate. The oil saturation of the specimen was reduced by gradually increasing the gas flow rate. The increment of gas pressure is presented in

supplementary section A. The decrease in oil saturation resulted in an increased gas permeability and decreased oil permeability. The steps described above were repeated until there was little or no measurable oil flow and the gas permeability was maximized.

Two mass flow controllers of different flow ranges were connected in parallel in the flow test system. As a result of this setup, it was possible to make the minute adjustments to the gas flow rate that are so frequently required for corrections to the visco-inertial flow.

Multiple flow experiments were conducted as part of the research. Variation in confining stresses were used to alter both the aperture size and flow path tortuosity. To investigate the role of viscosity, silicone oils with three viscosities were used. To study the influence of capillary number for two-phase flow through wellbore cement fracture, the capillary number of the simultaneous two-phase flow was also varied. The test matrix for simultaneous two-phase flow measurements is also indicated in Table 2.1.

Table 2.1 – List of specimens with the test matrix for simultaneous two-phase flow test. The non-wetting fluid was nitrogen in all tests.

Specimen	Wetting fluid	Confining stress (MPa)	Capillary number (Ca)	Purpose
S1-01	Silicone oil (Viscosity 5 cSt)	3.45	Low ($\log_{10}Ca = -10.98$)	3
S1-02	Silicone oil (Viscosity 10 cSt)	3.45	Low ($\log_{10}Ca = -10.98$)	1,2,3,4
S1-03	Silicone oil (Viscosity 10 cSt)	13.80	Low ($\log_{10}Ca = -10.98$)	1,4
S1-04	Silicone oil (Viscosity 10 cSt)	3.45	High ($\log_{10}Ca = -8.28$)	2
S1-05	Silicone oil (Viscosity 20 cSt)	3.45	Low ($\log_{10}Ca = -10.98$)	3
S2-01	Silicone oil (Viscosity 10 cSt)	3.45	Low ($\log_{10}Ca = -10.98$)	1,4
S2-02	Silicone oil (Viscosity 10 cSt)	13.80	Low ($\log_{10}Ca = -10.98$)	1,4

Notes:

1. Evaluating the role of aperture size in two-phase flow (changing confining pressure changes aperture size)
2. Evaluating the role of the capillary number on two-phase flow (the capillary number was controlled with flow rates)
3. Evaluating the role of viscosity ratio on two-phase flow (using silicone oils of different viscosity).
4. Evaluating the role of surface roughness on two-phase flow (using two different fractures).

Multiple gas flowrates were used for simultaneous two-phase flow testing of each specimen, while the liquid flowrate remains constant. As it takes some time for the HPLC pump to reach steady-state fluid phase flow, the test duration for certain flow tests lasted as long as two weeks. After every two-phase flow experiment, the fracture was cleaned by draining the fracture fluids with ultrapure nitrogen gas for 60 minutes inside the pressure vessel at 0.7 MPa confining stress (100 psig).

Data interpretation

At sufficiently low flow rates, the steady-state flow of any fluid phase (gas or liquid) is described by Darcy's law (Bear, 1972)

$$-\nabla P_{g/l} = \frac{\mu_{g/l} Q_{g/l}}{k_{g'/l} A} \qquad 4$$

where ∇P is the pressure gradient, μ is the dynamic fluid viscosity, Q is the volumetric flow rate, k is the permeability, and A is the flow cross-sectional area. The subscription *g'* refers to gas-phase (non-wetting phase) and *l* refers to liquid-phase (wetting phase). Here we refer to flow that follows Darcy's law as viscous flow.

The Equation 4 is directly applicable for liquid-phase but for a compressible fluid, the equation can be rewritten as

$$\frac{M\left(P_1{}^2 - P_2{}^2\right)}{2\rho z R \tau L} = \frac{\mu_g Q_g}{k_{g'} A} \qquad 5$$

where M is the molecular weight of gas, P_1 is the downstream gas pressure, P_2 is the upstream gas pressure, ρ is the gas density, z is the gas compressibility factor, R is the gas constant, τ is temperature, L is the length over which pressure drop takes place.

When the fluid flowrate exceeds some threshold, the relationship between flowrate and gradient becomes nonlinear. This divergence from Darcy's law at higher flow rates is a result of additional losses linked with the loss of inertial energy. In these experiments, the gas phase flow component includes inertial flow. To describe this non-Darcy or inertial effect on gas flow, Forchheimer (1901) presented the following equation

$$-\nabla P = \frac{\mu_g Q}{k_g, A} + \frac{\beta \rho {Q_g}^2}{A^2} \quad (6)$$

where the coefficient of inertial resistance, β, depends on both the type of fluid and the media (wellbore cement fractured) the fluid is flowing through (Geertsma, 1974; Tiss & Evans, 1989). Here, the term "visco-inertial flow" will refer to the flow regime that has a significant inertial flow component.

The transition from viscous to visco-inertial flow can be defined conceptually as a reduction in the overall pressure loss by a prescribed fraction, α. That fraction can be described mathematically from Equation 4 and 6,

$$\alpha = \frac{x_2 Q_g}{x_1 + x_2 Q_g} = \frac{F_o}{1 + F_o} \quad (7)$$

where $x_1 = \frac{\mu_g}{A k_g,}$ and $x_2 = \frac{\beta \rho}{A^2}$.

F_o is the Forchheimer number, which is a dimensionless ratio of pressure losses due to inertial forces to those attributed to viscous forces. F_o is used by researchers to describe the transition to visco-inertial flow (Ruth & Ma, 1992; Zeng & Grigg, 2006). The transition to strong inertial flow is defined at α = 10% or F_o = 0.11 in some recent studies (Zeng & Grigg, 2006; Zimmerman, Al-Yaarubi, Pain, & Grattoni, 2004).

For the steady-state flow of a real gas, Equation 6 can be reformed as below,

$$\frac{M\left({P_1}^2 - {P_2}^2\right)}{2\mu_g z R \tau L \rho Q_g} = \left[\frac{\rho Q_g}{A^2 \mu_g}\right]\beta + \frac{1}{A k_g,} \quad (8)$$

The above-mentioned form of the equation is advantageous for the data processing detailed in the subsequent paragraphs.

At substantially low flow rates, gas-phase flow can be affected by molecular slip phenomenon which arises due to the interaction between gas molecules and fracture walls (Klinkenberg, 1941). The measured gas-phase permeability can be related to the intrinsic or slip-corrected effective gas-phase permeability (k_g) as a linear function of reciprocal mean pressure (P_m)

$$k_{g'} = k_g\left(1 + \frac{b}{P_m}\right) \quad (9)$$

where b is known as gas slip factor.

For the two-phase flow test, the gas-phase flow was measured at a variety of pressure gradients. In order to interpret these data, slip and inertial effects had to be accounted for. Our interpretation of the gas-phase flow corrections follow the approach described by others (Anwar, Chojnicki, et al., 2019; Dranchuk & Kolada, 1968; Rushing, Newsham, Lasswell, Cox, & Blasingame, 2004).

The first step of the approach to data analysis is to plot the data as the permeability interpreted from Equation 5 as a function of the inverse of the mean pressure. This graph distinguishes between data from viscous and visco-inertial regimes. In the viscous regime, the data will adhere to Equation 9 and plot as a straight line, with the slope and intercept being equal to the slip factor and intrinsic or slip-corrected gas-phase permeability, respectively. In the visco-inertial regime, the inertial flow component causes the flow to deviate from a straight line. The transition flow rate, which is defined at α = 10%, is used to validate the grouping of data into two flow regimes.

The second step is to determine the coefficient of inertia and provide an additional estimate of the gas-phase effective permeability using only data from the visco-inertial regime. These data are first corrected for gas slip by replacing Equation 9 into Equation 8 and applying the correction generated in the first step.

$$\frac{M\left(1 + \frac{b}{P_m}\right)\left({P_1}^2 - {P_2}^2\right)}{2\mu_g z R \tau L \rho Q_g} = \left[\frac{\rho Q_g\left(1 + \frac{b}{P_m}\right)}{A^2\mu_g}\right]\beta + \frac{1}{Ak_g} \quad (10)$$

This equation is of the form $y = x\beta + (1/k_\infty)$, where y is the left-side of Equation 10 and x is the term in brackets on the right-hand side of Equation 10. Gas flow parameters measured at slightly different flow rates to generate (x,y) pairs, which can be plotted. The plotted data generate a straight line with a slope that is a function of the inertial coefficient β and an intercept inversely proportional to gas-phase effective permeability.

For convenience, the calculated permeability can be interpreted as a hydraulic aperture (h) using the cubic law (Witherspoon, Wang, Iwai, & Gale, 1980).

$$\mathrm{h}^3 = \frac{12k_{g/l}\mathrm{A}}{\mathrm{w}}, \qquad 11$$

where w is the fracture width.

Based on the uncertainties in the measured quantities, the maximum error in each set of reported permeabilities is about 10%.

Additional analytical measurements

Pressure mapping films were used to understand the variation in the contact area and flow path tortuosity of specimen group S1 due to the change in confining stress. These are very thin film (approx. 1 micron thick) and was placed in the fracture space prior to the application of confining stress inside the pressure vessel. The change in contact area owing to the change in confining stress was analyzed for specimens S1-02 and S1-03, where measurements of two-phase flow were performed for two confining stresses of 3.45 MPa and 13.8 MPa, respectively. To map the stress distribution in the fracture space as a result of applied confining stresses, two different Fuji pressure-sensitive film models were used. Multiple colors are associated with a variety of pressure ranges, depending on the manufacturer of the film. The hue of each color is calibrated to the amount of stress exposed, and any change in film color indicates the pressure contact zone. The white tint (unaltered) indicates areas with no contact pressure, indicating zones without contact. The low pressure zone may also be out of contact during fluid movement, since the fluid's pore pressure will prop open a section of the fracture region to complete the flow in the region where the film received the lowest pressure. A computer application for image processing (Image J) is used to calculate the change in contact area from the ultraviolet (UV) images of the pressure-sensitive film of the specimens S1-02 and S1-03 experiencing two different confining stresses.

Brookfield RST-coaxial cylinder Rheometer was used to measure fluid viscosity in the laboratory. The device calibration was verified using fluids of known viscosity, prior to each viscosity measurement. The viscosities of the test fluids were measured multiple

times (at least four measurements each time) immediately before and after the flow test, at the same room temperature.

To evaluate the flow capillary number, the interfacial tension (σ) between the silicone oil and the nitrogen gas is required. We have used an automated force tensiometer (Sigma 700 by Biolin Scientific) at the Los Alamos National Laboratory to directly measure the interfacial tension of the fluid-fluid system. A computer program named “OneAttention” by Biolin Scientific was used to reduce the tensiometer data and calculate the interfacial tension.

The roughness coefficient of the fracture surface was evaluated using a mechanical surface profiler, developed by the Geomechanics laboratory at The University of New Mexico .The surface profiles of the specimens were recorded using a mechanical profiler developed at the University of New Mexico (Anwar, Hatambeigi, & Stormont, 2019). The fracture surface profile was documented in terms of statistical parameters commonly used to quantify roughness of the fractures - average roughness (R_a), root mean square roughness (R_{rms}), maximum peak-to-mean height (R_p) and peak asperity height (ξ).

Development of a new model:

A mathematical model suited for wellbore leakage is developed based on a thorough theoretical analysis of two-phase flow dynamics. As is customary, the developed model includes unknown parameters or coefficients. These parameters are then empirically determined using experimental results. The model is optimized and validated by comparing theoretical predictions to findings from experiments

3. Results and discussions

The two-phase flow through wellbore cement fractures is shown to be affected by the confining stress, viscosity ratio, and capillary number. All test results were corrected for non-linear (i.e., visco-inertial) flow as necessary and interpreted in terms of either relative permeability (two-phase flow) or hydraulic apertures (single-phase flow) of the fractures.

A list of the flow test performed, test condition with the details of the fluids used and the intrinsic permeability of the sample is presented in Table 3.1.

Simultaneous two-phase flow tests were undertaken after the specimen was saturated from the single-phase flow test. Oil saturation was not measured during the two-phase flow testing due to limitations of test system. As such, a qualitative scale for oil saturation is given with the relative permeability data to aid in the understanding of the data.

Table 3.1– The fluid flow tests performed and the flow test conditions. The intrinsic permeability of the samples is obtained from single-phase silicone oil flow test. The non-wetting fluid was nitrogen in all tests.

Test ID	Viscosity of silicone oil (cSt)	Confining stress (MPa)	Viscosity ratio (M)	Capillary number ($\log_{10} Ca$)	Intrinsic permeability (m^2) of the fracture
S1-01	5	3.45	3.5	-10.98	7.03E-14
S1-02	10	3.45	1.7	-10.98	7.57E-14
S1-03	10	13.8	1.7	-10.98	2.25E-14
S1-04	10	3.45	1.7	-8.28	9.25E-14
S1-05	20	3.45	0.8	-10.98	5.38E-14
S2-01	10	3.45	1.7	-10.98	1.61E-12
S2-02	10	13.8	1.7	-10.98	1.03E-13

The table displays the measured effective permeability and the fracture permeability is many orders of magnitude greater than the cement matrix permeability (Anwar, et al., 2019). Hence, it is safe to assume that the tabulated effective permeability is equal to the fracture permeability.

3.1 Effect of confining stress

The relative permeabilities of each fluid phases are measured from simultaneous two-phase flow tests through wellbore cement fracture at two different confining stresses –

3.45 MPa (500psig) and 13.8 MPa (2000 psig). Four flow experiments (Table 3.2) are conducted to collect experimental data on how changes in confining stress affect the two-phase flow. As presented in Table 3.2, at the same confining stress, the hydraulic aperture of specimens S1-02 and S1-03 is less than the specimens S2-01 and S2-02. The experimentally obtained hydraulic apertures of both fractures cement samples is tabulated below,

Table 3.2 – Hydraulic aperture of two different cement fractures (Samples - S1 and S2) at two different confining stresses obtained from single-phase silicone oil flow test.

Specimen ID	Applied confining stress	Mean hydraulic aperture (μm)
S1-03	13.8 MPa	27
S1-02	3.5 MPa	40
S2-02	13.8 MPa	79
S2-01	3.5 MPa	110

The relative permeability measurements of two phases for different apertures of the cement fracture along with the commonly used models – X-curve, viscous coupling, and porous media approach (Corey's model) are presented in Figure 3.1. The variation in confining stress (from 3.45 MPa to 13.8 MPa), reduces the hydraulic aperture as well increase the contact area, which affects the flow path tortuosity. From Figure 3.1, it is clear that the relative permeabilities do not follow the X-curve, which indicates strong phase interference.

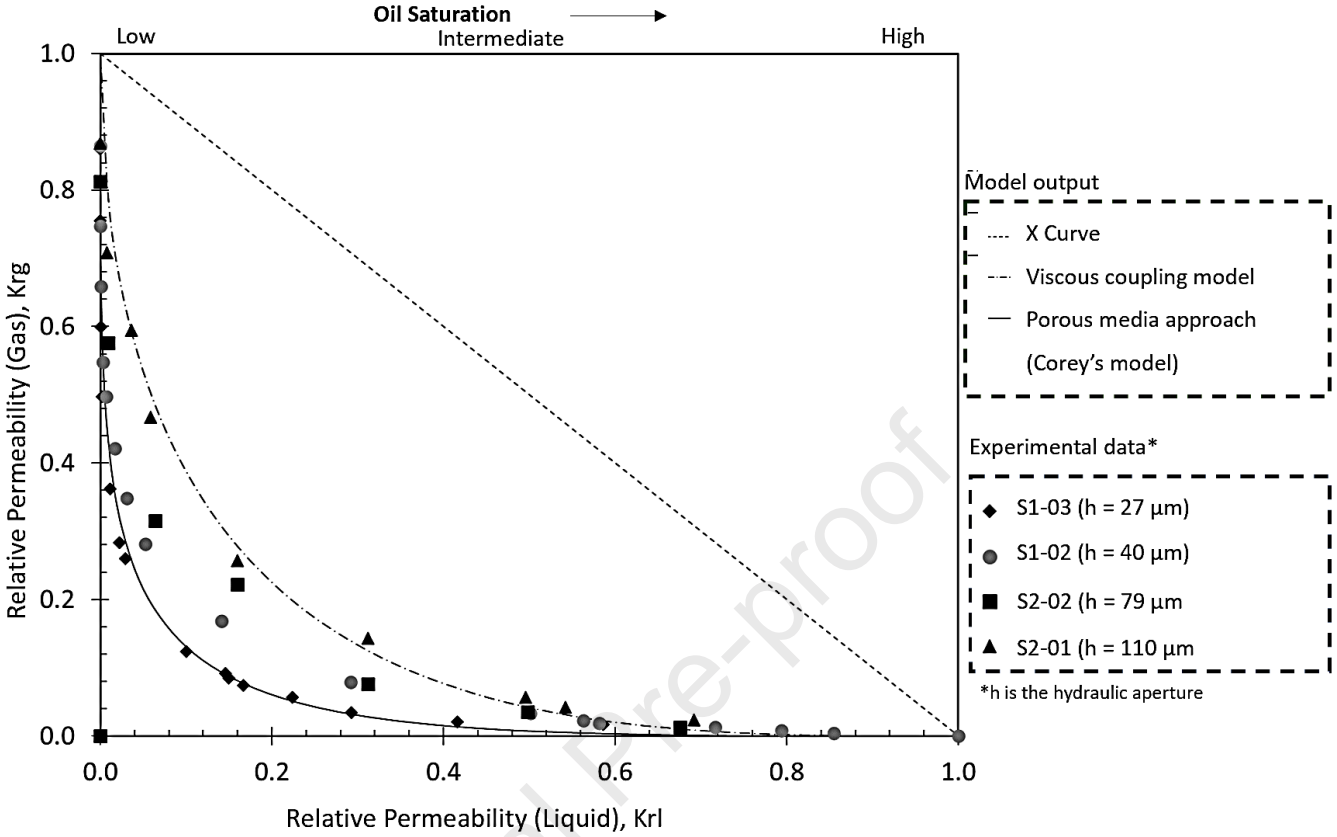

Figure 3.1 – The relationship between wetting (l) and non-wetting (g) relative permeabilities (Kr) for different fracture apertures (experimental data and model output)

The relative permeabilities for the specimen S1-03 with relatively smaller fracture aperture (hydraulic aperture of 27 µm) can be reasonably described by Corey's model. In such cases, the fracture behaves like a porous media, where the competition for pore occupancy is controlled by capillary pressure.

The relative permeabilities of specimens S1-02 and S2-02 with a hydraulic aperture of approximately 40 m and 79 m, respectively, fall between the viscous coupling model and the porous media model.

The results for S1-02 (h = 40 µm) indicate, a deviation from the Corey's model at intermediate saturation, which suggests that simultaneous sharing of pore space by fluids can occur to a certain extent for two-phase flow through a fracture with this hydraulic aperture (40 µm). Such interaction between the fluid phases is not obvious at high or low

oil saturation. At low or high oil saturation, the fracture flow can be described by Corey's model.

The test results for S2-02 (79 μm) are intermediate between the porous and viscous coupling model. This implies that for intermediate oil saturations, simultaneous sharing of pore space by fluids can occur to a certain extent for two-phase flow through a relatively large hydraulic aperture (79 μm), which can be partially explained with the viscous coupling model.

The relative permeabilities of specimen S2-01 with the larger fracture aperture (hydraulic aperture of about 110 μm) can be reasonably modeled using viscous coupling model. In such cases, the fracture flow resembles to the flow through a pipe, where both fluid phases simultaneously flow through the fracture network by balancing the viscosity with fluid inertia, body forces, and pressure gradient with strong interaction or viscous coupling between the phases.

As presented in Figure 3.1, multiple relative permeability measurements are made at about same saturation stage for three different viscosity ratios. Using Student's t-statistics, it was observed that the obtained P-values were less than 0.05 for the viscosity ratios comparisons. The obtained P-values were substantially low (< 0.02) for each of the specimens. These results suggest that at 0.05 level of significance, the values of each group are different.

Variation in contact area

Alteration in the contact area, which also affect the flow path tortuosity by affecting the flow path geometry, are able to affect the relative permeabilities of a fracture. The processed images (using TOPAQ pressure analysis system performed by Sensor Products Inc. NJ, USA) of the pressure sensitive films under Ultra-Violet (UV) light were obtained to understand the variation in the contact area for two confining stresses of 3.45 MPa and 13.8 MPa, respectively. The UV image of two pressure sensitive films, for specimens S1-02 and S1-03, are presented in Figure 3.2. Figure 3.2 demonstrates that the viscous coupling effect in the two-phase flow through relatively low-permeability

wellbore cement fractures is perhaps diminished by the increasing contact area resulting from larger confining stress.

The increase in contact area is assessed using pressure-sensitive films placed in the fracture space of the specimen within the pressure vessel. Using both the Topaq film testing equipment and ImageJ analysis, the fracture contact area at 3.45 MPa (500 psig) is determined to be 53.35 cm^2 (8.27 in^2). For specimen S1-03, increasing the confining pressure to 13.8 MPa (2000 psig) increased the the contact area by 13.2% to 60.39 cm^2 (9.36 in^2) at. According to the results, an increase in confining stress increases the fracture contact area in wellbore cement fracture.

Previously, fracture contact area measurements were conducted using pressure-sensitive paper (Duncan & Hancock, 1966) and deformable film (Bandis, Lumsden, & Barton, 1983; Iwai, 1976). All experimental studies have demonstrated that contact area rises with confining stress and is material-dependent.

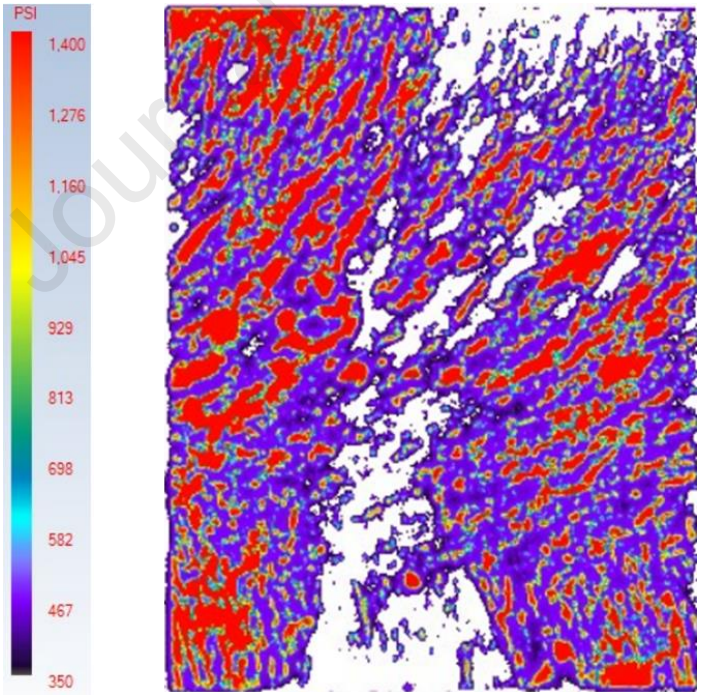

(a)

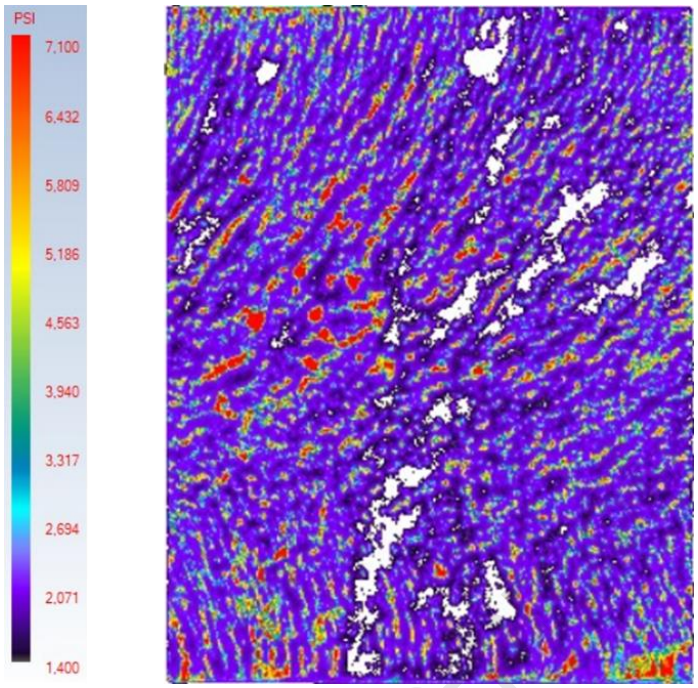

(b)

Figure 3.2 – The ultraviolet (UV) images of the pressure sensitive film from cement fracture of specimens (a) S1-02 at confining stress = 3.45 MPa (b), and S1-03 at confining stress = 13.8 MPa, illustrating that the total contact area of the fracture increases with an increase in applied confining stress.

3.2 Effect of viscosity ratio

We studied the dependency of the relative permeabilities on the viscosity ratio between fluid phases. The relative permeability measurements of two phases for fracture of same aperture (at a confining stress of 3.45 MPa) for silicone oils of three different viscosities along with the commonly used models – X-curve, viscous coupling, and porous media approach (Corey's model) are presented in Figure 3.3. In general, the experimental findings (Figure 3.3) indicate that the effect of viscosity ratio cannot be ignored for two phase flows through a variable aperture fracture, and that increasing the viscosity ratio (M) from 0.8 to 3.5 reduces interference and shifts the relationship away from the porous media (Corey's) model and toward the viscous coupling model.

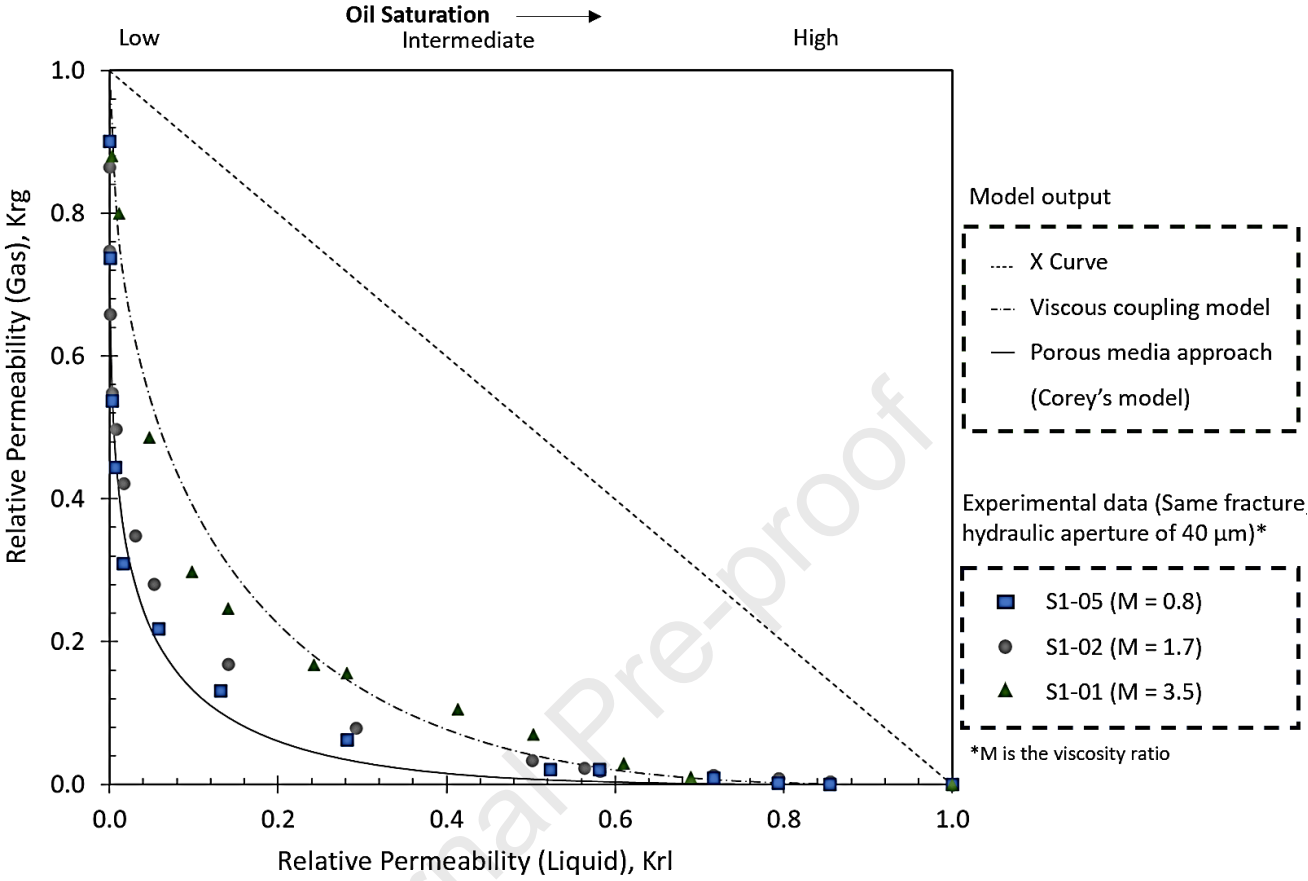

Figure 3.3 – The relationship between wetting (l) and non-wetting (g) relative permeabilities (Kr) for different viscosity ratios (experimental data and model output)

As observed in Figure 3.3, the presence of strong phase interference is obvious for all three values of M (0.8, 1.7, and 3.5). For the given range of viscosity ratios, the X-curve is not effective in estimating the relationship between the relative permeabilities.

The phase interference increases with a decrease in the viscosity ratio. The relative permeabilities for the viscosity ratio of 0.8 or less may be reasonably described using Corey's model or porous media approach.

The relative permeabilities for the fracture with the viscosity ratio of 1, falls between the viscous coupling and Corey's model. The outcome suggests that, silicone oil (of relatively lower viscosity) is removed by gas from the fracture with some immobile oil in the fracture,

while most of the space in occupied by gas. As such, where simultaneous sharing of pore space by fluids reduces, and at some portion of the flow network the competition for pore occupancy is controlled by capillary pressure, behaving like a porous media, making the two-phase flow complex.

The relative permeability measurements of gas-liquid two-phase for viscosity ratio of 3.5 shows that at higher to intermediate saturation, the viscous coupling model may reasonably estimate the permeability of the individual phases for intermediate saturation. A deviation from the viscous coupling model at lower saturation is observed, suggesting an alteration in fluid phase interaction or coupling, which can be caused by the flow through the porous cement adjacent to the fracture surface.

As presented in Figure 3.3, multiple relative permeability measurements are made at about same saturation stage for three different viscosity ratios. Using Student's t-statistics, it was observed that the obtained P-values were less than 0.05 for the viscosity ratios comparisons. The obtained P-values were substantially low (< 0.02) among the viscosity ratios - M = 0.8, M = 1.7, and M=3.5. The statistical analysis suggest that at 0.05 level of significance, the values of each group are different.

3.3 Effect of flow capillary number

In this study. we have used the conventional capillary number Ca ($=\mu_l v_l/\sigma$), where $v_l = Q_l/A_c$, Q_l is the gas phase flow rate, and A_c is the cross-sectional area of the liquid inlet (Lenormand, Touboul, & Zarcone, 1988; C. Zhang, Oostrom, Wietsma, Grate, & Warner, 2011). Lower capillary numbers indicate that the flow is affected more by capillary forces than viscous forces.

The measured interfacial tension (σ) between the silicone oil and gas is 20.24 ± 0.5 mN/m. Ca for specimen S1-02 ($\log_{10}Ca = -10.98$) is roughly two orders of magnitude lower than Ca for specimen S1-04 ($\log_{10}Ca = -8.28$).

The relative permeability measurements of two fluid phases for wellbore cement fracture of same aperture for two different fluid flow rates, that translate in two different Ca along with the commonly used models – X-curve, viscous coupling, and porous media approach

(Corey's model) are presented in Figure 3.4. In general, the findings (Figure 3.4) suggest that the Ca affects the two-phase flows through the variable aperture fracture used in this investigation.

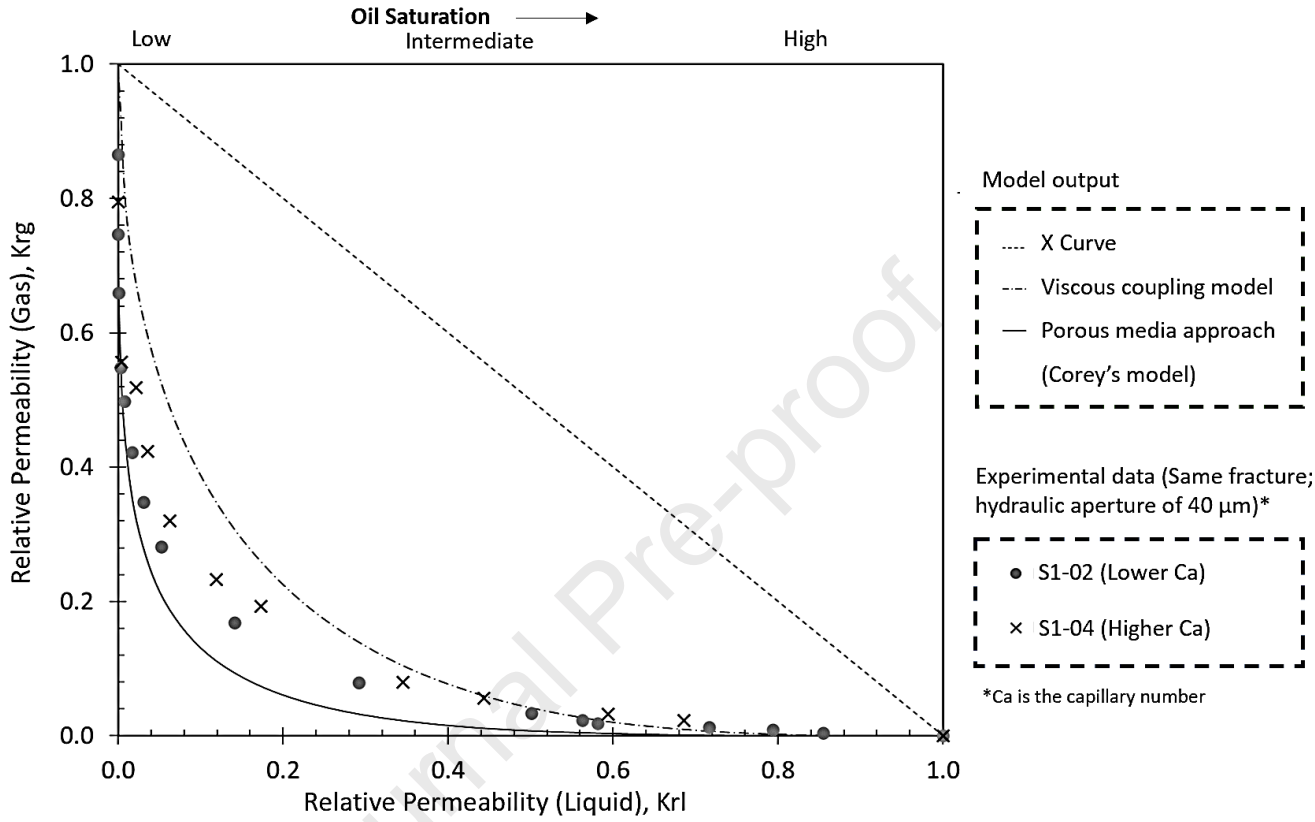

Figure 3.4 – The relationship between wetting (l) and non-wetting (g) relative permeabilities (Kr) for different capillary number (experimental data and model output)

As observed in Figure 3.4, the presence of strong phase interference is obvious for all two values of Ca. The X-curve is not an effective model for estimating the relationship between the relative permeabilities.

The relative permeabilities for the fracture with the lower capillary number cannot be fully modeled using either the viscous coupling or Corey's model. The outcome suggests that, for two-phase fluid flow through the wellbore cement fractures with characteristic geometry of void depends on the value of Ca.

The relative permeability measurements of gas-liquid two-phase for higher Ca shows that at higher to intermediate saturation, the viscous coupling model may reasonably estimate

the permeability of the individual phases for intermediate saturation. A deviation from the viscous coupling model at lower saturation is observed, suggesting an alteration in fluid phase interaction or coupling, which can be caused by the flow through the porous cement adjacent to the fracture surface.

As presented in Figure 3.4, multiple relative permeability measurements are made for each saturation for two different Ca. Using Student's t-statistics, it was observed that the obtained P-values were less than 0.05. The obtained P-values were substantially low (< 0.02) for higher Ca in comparison to lower Ca. These results suggest that at 0.05 level of significance, the values of each group are different.

3.4 Gas Slippage factor

As discussed in previous section, the gas slippage effect or the Klinkenberg effect of gas-phase flow exists in the two-phase flow through wellbore cement fracture. Two different empirical relationships between the gas slippage factors and the gas-phase effective permeasbility is ovserved for two different saturation ranges.

For relatively higher saturation, with lower realtive permeability of gas phase ($K_{r,g}$ < 0.1), the gas slippage factors (b) are plotted as a function of measured effective gas-phase permeabilities (K_g) and is presented in Figure 3.5. The best-fit straight line through the data yields,

$$b = C_b \, K_g{}^{-0.19} \qquad 12$$

Where the coefficient, C_b = 14.38 kg m$^{-0.62}$ s^{-2} and the units of b and K_g are in Pa and m^2, respectively.

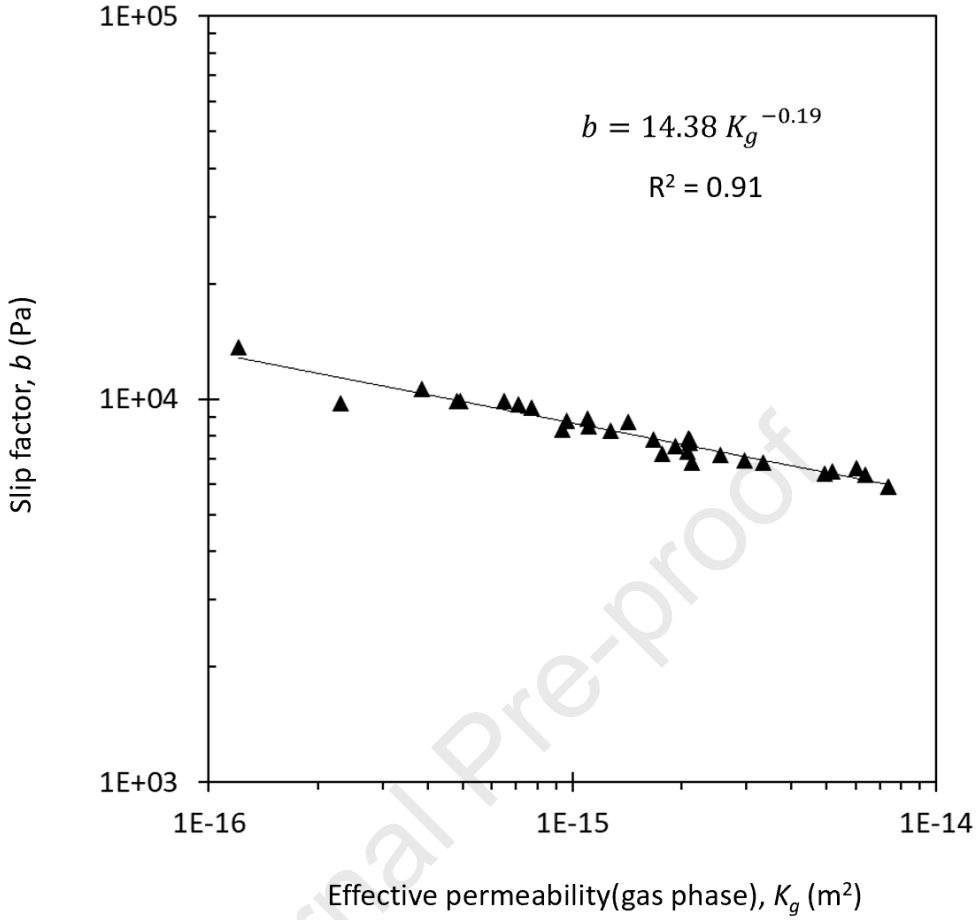

Figure 3.5 - Gas slippage factors as a function of measured effective gas permeabilities for two-phase flow through wellbore cement fracture at relatively higher saturation -.

A previous study (Reinecke & Sleep, 2002) that included a summary of earlier research investigated the variance of the Klinkenberg coefficient for air for unsaturated flow in porous media. They developed an equivalent correlation for the the Klinkenberg parameter for unsaturated flow conditions as a function of effective gas permeability.

For a higher gas relative permeability (of about 0.3) the above correlation is about the same as Heid et al. (1950) (Heid, McMahon, Nielsen, & Yuster, 1950). The best-fit straight line through the data yields (Figure 3.6),

$$b = C_b\ K_g^{-0.40} \qquad 13$$

where the coefficient, C_b = 0.28 kg m$^{-0.2}$ s^{-2} and the units of b and K_g are in Pa and m^2, respectively.

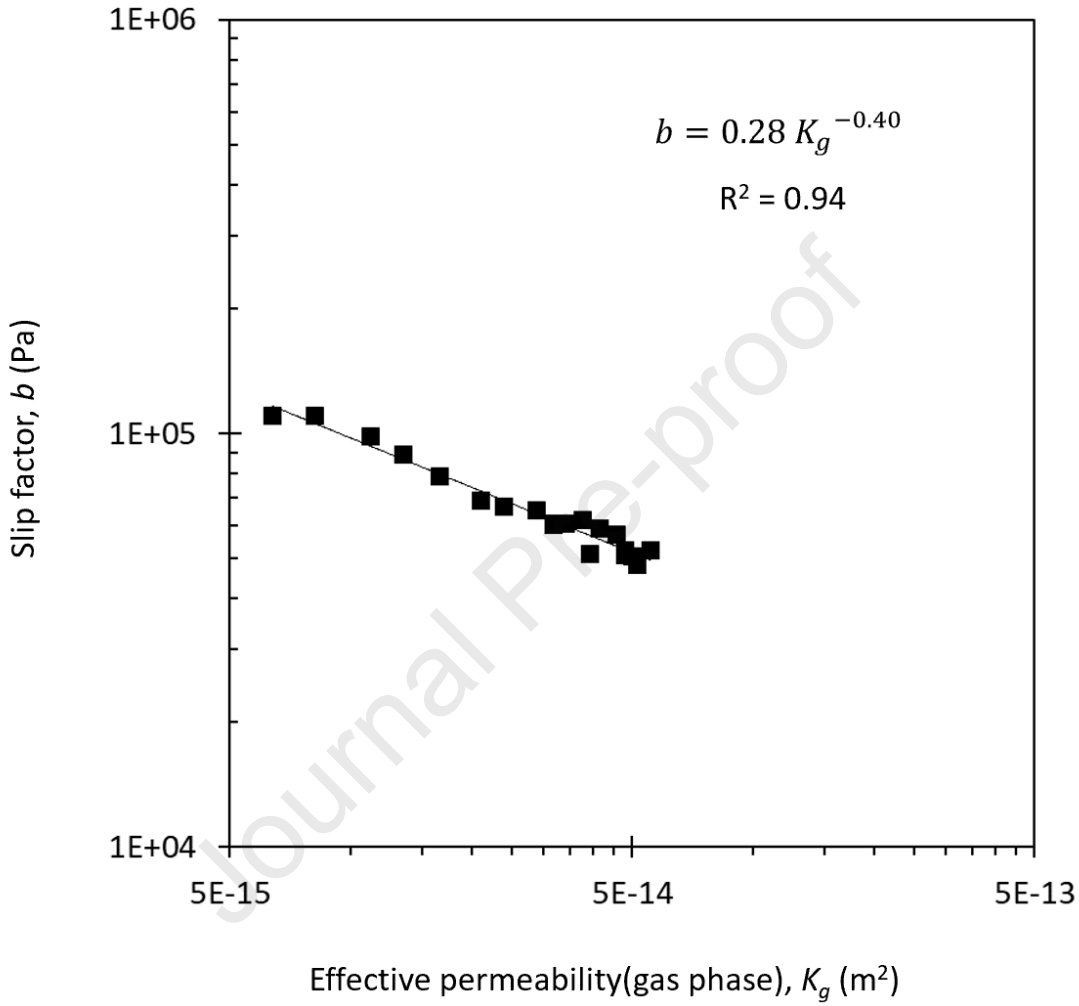

Figure 3.6 - Gas slip factors as a function of measured effective gas permeabilities for two-phase flow through wellbore cement fracture at relatively lower saturation.

As the effective permeability decreases, the above correlation gives a smaller value of the Klinkenberg factor, or a smaller effect on the permeability, than the correlations established for single-phase gas flow through porous media (Heid et al., 1950; Jones & Owens, 1980). This difference may be due to the fact that liquid preferentially blocks the

pathways with smaller diameter in the variable aperture fracture, which have the most influence on gas slippage.

Empirical relationships between gas slippage factor and permeability derived from the previous studies are presented in Table 3.3 for comparison to the present study. The theoretical value of the exponent is -0.5 for an assumed geometry of uniform cylindrical capillaries with single-phase flow; empirical exponent values less than -0.5 have been attributed to actual pore geometries differing from uniform cylindrical capillaries (Heid et al., 1950)

Table 3.3 - Empirical equations for estimating gas slippage factor (b)

Correlations	Equation	Effective gas permeability range (m^2)	Flow type	Material
Heid et al.	$b = 0.11\ K_g^{-0.39}$	10^{-22} to 10^{-16}	Single-phase	Sandstone core
Jones & Owens	$b = 0.98\ K_g^{-0.33}$	10^{-23} to 10^{-18}	Single-phase	Low permeability sands
Reinecke & Sleep	$b = 50.8\ K_g^{-0.24}$	10^{-17} to 10^{-15}	Two-phase	Silica Flour
Current study	$b = 14.38\ K_g^{-0.19}$	10^{-17} to 10^{-15}	Two-phase (Higher oil saturation)	Wellbore cement fracture
	$b = 0.28\ K_g^{-0.40}$	10^{-15} to 10^{-13}	Two-phase (Lower oil saturation)	

Notes

1. The equations (Heid et al., 1950; Jones & Owens, 1980; Reinecke & Sleep, 2002) have been adjusted for nitrogen gas (Ho & Webb, 2006) and converted to effective permeabilities for comparison to the measurements reported here.
2. The units of b and K_g are in Pa and m^2, respectively.

In this experimental study, we did not observe the gas slippage or Klinkenberg effect for the two-phase flow for specimen S2-01, where the fracture permeability is about 10^{-12} m^2. The gas slippage effect is also not measurable where the gas phase relative

permeability is about 0.9 i.e. the fracture oil saturation is significantly low or the effective gas permeability is about 10^{-13} m^2 or higher. To further verify, we have measured the smallest pore sizes in the fracture network using the Young Laplace equation for all of the flow measurements. We have also estimated the mean free path of nitrogen gas at different pore pressure. The ratio of the mean free path and the smallest pore of the fracture network, which is also known as the Knudsen number, was compared. The ratio was less than 0.01, which suggest that for single-phase gas flow or for two-phase flow where the saturation is about zero, the wellbore cement fracture network used in this study is free from gas slippage effect (Heller et al., 2014b).

3.5 Fracture surface roughness

The relative permeability of cement fracture is significantly influenced by the roughness of the fracture. It is evident that the geometry of the fluid flow path within cement fractures is somewhat dependent on the roughness of the fracture surface. The cement fractures in the wellbore are not smooth and contain uneven projections, which we will refer to as "asperities" in this article. The asperities can vary in amplitude (height) and location.

Researchers found that the asperities in the fracture could act as a localized blockage and interfere with the flow of fluid through the fracture (Raven & Gale, 1985; Z. Zhang & Nemcik, 2013). Consequently, a relatively rough fracture surface with two-phase fluid flow might result in increased energy loss, thereby increasing the degree of nonlinearity.

We have measured the surface profiles for the samples used in this study and reported in terms of statistical parameters commonly used to quantify fracture roughness. These parameters are defined in Equations 14 through Equation 17 (Bhushan, 2001; Guerrero, Reyes, & González, 2002; Wang et al., 2016) –

$$R_a = \frac{1}{n}\sum_{i=1}^{n}|Z_i - \bar{Z}| \qquad 14$$

$$R_{rms} = \sqrt{\frac{1}{n}\sum_{i=1}^{n}(Z_i - \bar{Z})^2} \qquad 15$$

$$R_p = Max\,|Z_i - \bar{Z}| \quad (16)$$

$$\xi = Z_{max} - Z_{min} \quad (17)$$

where n is the number of data points forming a profile line, *i* is the index of the points, *Zi* is the asperity height of each point, $\bar{Z}$ is the mean line height, Z_{max} and Z_{min} are the maximum and minimum asperity heights. The fracture roughness parameters are summarazied in Table 3.4, which indicates that the specimen S2 (S2-01 to S2-02) has the roughest fractured surface, as indicated by all four parameters, in comparison to specimen S1 (S-01 to S1-05).

Table 3.4 - Roughness parameters of the wellbore cement fractures used in this experimental study

Specimen ID	**S1**	**S2**
Average Roughness, R_a (mm)	0.88	1.26
Root mean square roughness, R_{rms} (mm)	0.48	0.72
Maximum peak to mean height, R_r (mm)	2.52	3.82
Peak asperity height, ξ (mm)	3.36	6.34

The specimens are exposed to fluids as well as experienced confining stresses during the flow test, there is a possibility that some of the asperities may have altered from its original condition.

Coefficient of inertial resistance

In most studies, it is shown that *β* (Equation 6**Error! Reference source not found.**) is a function of geometrical feature of the medium. The geometrical features are almost similar for the fractured specimens tested in this study. The gas or non-wetting fluid phase will encounter localized obstructions or energy losses caused by the simultaneous liquid or wetting phase fluid flow at different saturations. Hence the value of *β* varies for gas-phase

flow at different saturation or gas-phase relative permeability. When visco-inertial flow is involved, the value of the inertial coefficient is also required in addition to the relative permeability of the fluid phase. The variation of flow nonlinearity through the wellbore cement fracture for different relative permeabilities has been experimentally observed and an empirical relationship between the coefficient of inertial resistance and the relative permeability has been developed.

We have observed two different empirical relationships between the coefficient of inertial resistance (*β*) and gas-phase effective permeability for two different saturation ranges. The measured values of *β* for different gas-phase permeability is plotted as a function of gas-phase effective permeability for two different saturation zone – relatively higher saturation with where the realtive permeability of gas phase is lower ($K_{r,g}$ less than 0.1 for specimen S1 and $K_{r,g}$ less than 0.2 for specimen S2) and relatively lower saturation where the realtive permeability of gas phase is lower ($K_{r,g}$ > 0.2). The These data are fit to the empirical equation

$$\beta = m\, K_g{}^{-n} \qquad 18$$

where the unit of β is 1/m, and K_g is m^2.

For relatively higher saturation, the best-fit straight line through the plot of coefficient of inertial resistance (*β*) vs. gas-phase effective permeability (Figure 3.7) yields,

$$\beta = m\, K_g{}^{-2.44} \qquad 19$$

Where the coefficient, m = 1 x 10^{-18} m$^{3.88}$

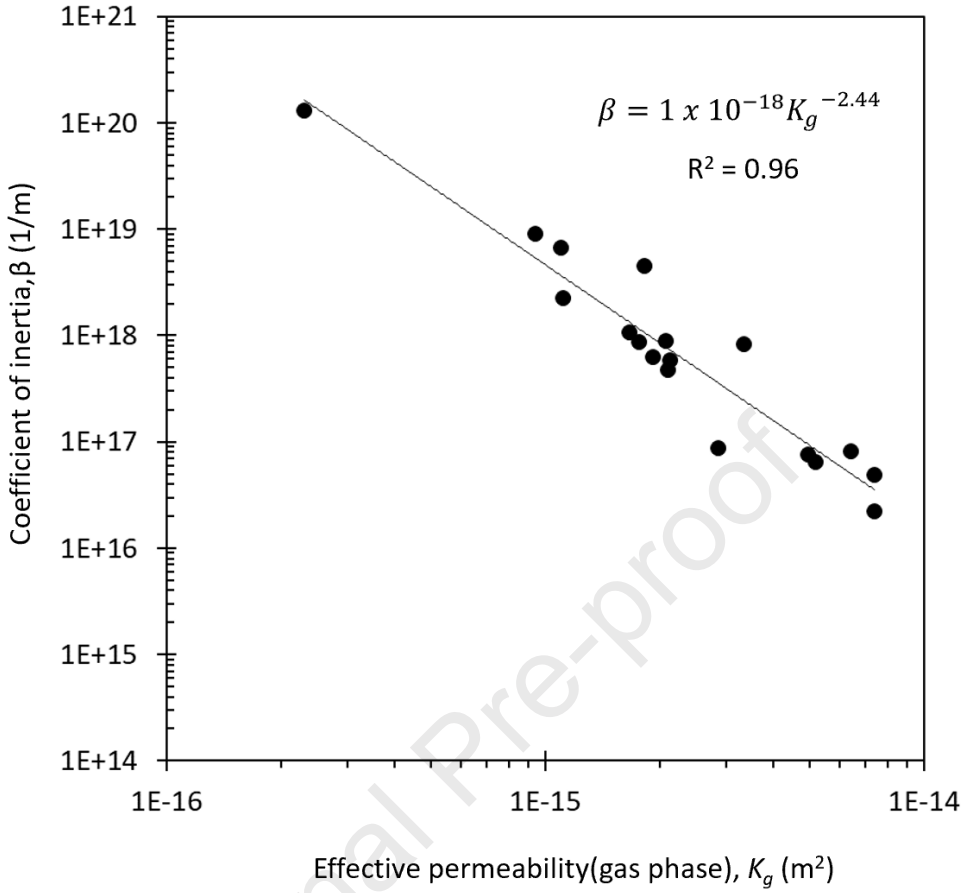

Figure 3.7 - Coefficient of inertial resistance (*β*) as a function of measured effective gas permeabilities for two-phase flow through wellbore cement fracture at relatively higher saturation - with lower realtive permeability of gas phase, $K_{r,g}$ less than 0.15.

For relatively lower saturation, the best-fit straight line through the plot of coefficient of inertial resistance (*β*) vs. gas-phase effective permeability (Figure 3.8) yields,

$$\beta = m\ K_g{}^{-4.09} \qquad 20$$

Where the coefficient, $m = 4\ x\ 10^{-26}$ $m^{7.18}$

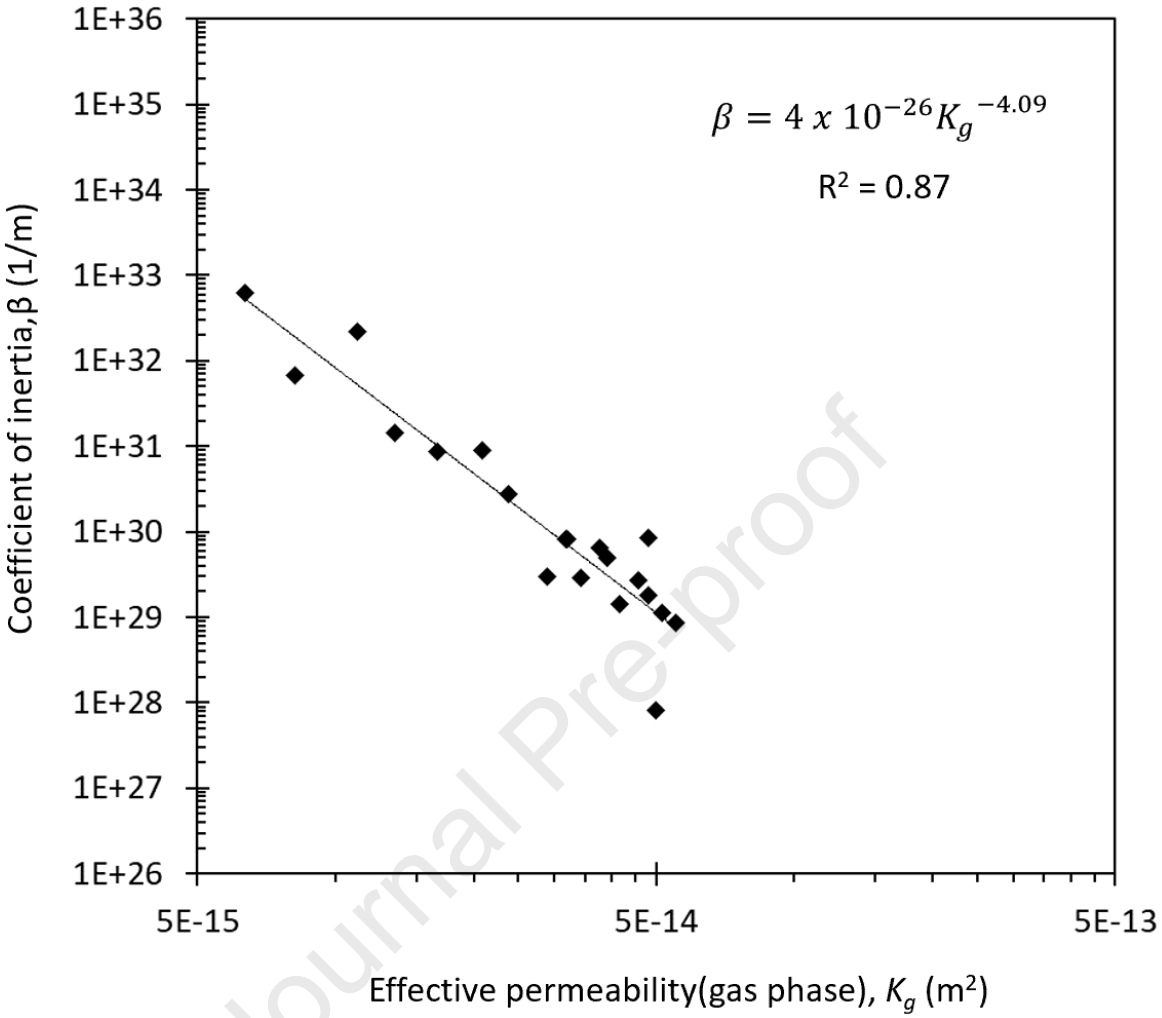

Figure 3.8 - Coefficient of inertial resistance (*β*) as a function of measured effective gas permeabilities for two-phase flow through wellbore cement fracture at relatively lower saturation - with higher realtive permeability of gas phase.

At lower effective permeability of gas (relatively higher saturation), the above correlation gives a smaller value of the *β*, or a smaller effect on the permeability, than the correlations established for single-phase gas flow through porous media. This difference may be due to the fact that liquid will preferentially occupy the pathways with smaller diameter in the variable aperture fracture, which have the most impact on the inertial resistance.

The regression coefficients m and n are listed in Table 3.5, and were found for each test individually as well as for the entire data set for all samples. The coefficient n varies in a

narrow range among the test conditions, while the value of m varies by an orders of magnitude.

Table 3.5 – Best fit parameters of Equation 18

Fracture saturation	m	n
Medium to high	$1\ x\ 10^{-18}$	2.44
Low to medium	$4\ x\ 10^{-26}$	4.09

We have provided, for the sake of simplicity, the relative permeability of gas, which also serves as an indication of saturation level. However, the coefficient of inertial resistance, is connected to the Critical Reynolds Number, a threshold at which the nonlinear behavior of the gas phase begins.

The higher saturation zone with equation 19 for specimens group S1 is observered for relative gas permeability less than 0.1 which was different for specimen group S2, where the equation providing lower coefficient of inertial resistance (Equation 20) is valid for relative gas permeability up to 0.2. It could be due to the unique surface roughness features of specimen group S2, where the fracture's undulations-created small passageways are occupied by the liquid phase.

Identical behavior has been observed in rock fractures with m differing by up to two orders of magnitude, which has been attributed to changes in the surface properties of the rock fracture's expressions (Y.-F. Chen et al., 2015; Cooke Jr, 1973; Zhou et al., 2015) .

3.6 A new model for wellbore cement fracture

The experimental study suggests that existing models or approaches cannot fully predict the relative permeabilities for the cement fractures included in this study. These findings point to the need for a new model ~~to~~ for two-phase flow through cement fractures.

Inside the fracture in the cement, there might be a wide range of pore diameters. When two fluids are flowing through a fracture, the size of the pores the fluids are passing through determines whether or not one fluid will interfere with the flow of the other. As such, both porous medium approach and viscous coupling model are useful to predict two-phase flow through variable aperture fracture. We suggest a new mathematical

model by integrating the existing effective models to account for the flow phenomenon occurs in both porous media (Brooks & Corey, 1964; Burdine, 1953) as well as in pipe or tube (Fourar & Bories, 1995; Lockhart & Martinelli, 1949) to produce physically meaningful trends for the relative permeabilities of immiscible two-phase flow through wellbore cement fracture. We have also assumed that due to the presence of the asperities in wellbore cement fracture, there will not be any parallel flow channels of almost equal flow rate (typically described by X- model) (Maloney & Doggett, 1997; Romm, 1966).

The mathematical model is comprised of two-parts – (i) porous medium approach, developed by combining the retention model (capillary pressure vs. fluid saturation) and permeability model for porous medium; and (ii) viscous coupling model, based on a pipe flow approach. The mathematical form is given below,

$$Kr_g = a(1-S)^A(1-S^B)^C + (1-a)\left\{(1-S)^3 + \frac{3}{2}\frac{\mu_g}{\mu_l}S(1-S)(2-S)\right\} \quad (21)$$

$$Kr_l = a(S)^D + (1-a)(3-S)\frac{S^2}{2} \quad (22)$$

Where *S* is the wetting fluid saturation, and μ is the dynamic viscosity of fluid. The parameter a is introduced to account for a fraction of relative permeability that will follow the porous media approach. The remaining relative permeability can be explained using the viscous coupling model. The value of a can vary between 0 to 1, a = 0 for two-phase flow completely following the viscous coupling model, and a = 1 for phase flowing at its own path without impeding the flow of the other phase.

The exponents A,B and D are introduced to account for the connectivity and the tortuosity of the flow network (Brooks & Corey, 1964; Burdine, 1953; Mualem, 1976). The values of the exponents depend on the parameters of the respected retention and permeability models. For our study we have used the Brooks Corey's retention model (Brooks & Corey,

1964) together with the Burdine's permeability model (Burdine, 1953), where the exponents A = 2; B = (2+λ) / λ; and D = (2+3 λ) / λ. Theoretically λ can be any positive value and a characteristic constant of the medium. The value of λ is large for the fracture media, ranging from 1.6 to 3.6, with flow network incorporating uniform pore sizes and decreases for a fracture with a wide range of pore sizes. Brooks and Corey associated λ with the distribution of the pore sizes.

Equations 21 and 22 show that, besides saturation, the fluid relative permeability depends on the viscosity ratio and capillary number. The relative permeability also depends on the connectivity and the tortuosity of the fracture network. Corey's model (Corey, 1954), commonly used in petroleum engineering for approximating relative permeability, can also be considered as a special case of the porous medium approach for λ = 2.

The portion of equations 21 and 22, handling the viscous coupling model, is adopted by combining the simplified form of Stokes equation for simultaneous fluid flow through parallel plates of small aperture (Fourar et al., 1993, 1991; Lockhart & Martinelli, 1949) and Darcy's law for fluid flow. This is to account for the interaction of fluids such as film flow, discontinuous bubbles, etc. at certain locations of the fracture.

The exponent C is to account for the capillary model and depends on the ratio between the viscous force to the capillary force for the two-phase flow (Burdine, 1953; Mualem, 1976). Finally, the parameters a, λ and C are evaluated using least square minimization, using a python script, from the experimentally obtained relative permeability data and presented in Table 3.6.

Table 3.6 - The parameters a, λ and C obtained from experimentally obtained relative permeability data

Specimen	a	λ	C
S1-01	0.42	1.92	0.9
S1-02	0.80	1.90	1.2
S1-03	0.96	2.10	1.0
S1-04	0.72	2.00	2.8
S1-05	0.92	1.60	1.4
S2-01	0.12	2.60	1.5
S2-02	0.55	3.62	1.5

As previously described in this section, the experimentally observed data indicate that the parameter a ranges from 0 to 1. The minimum value of a is found for specimen S2-01 (a = 0.12), where the two-phase flow predominantly follows the viscous coupling model. The maximum value of a = 0.96 for specimen S1-03 indicates that the two-phase flow follows the porous media approach, i.e., each phase flows along its own path without impeding the flow of the other phase. As observed in Table 3.6, the evaluated values of λ are lower for the specimen group S1 than the rougher specimen group S2. The highest value of λ is observed for the specimen S2-02, where the flow distribution is more tortuous, with a greater variation in channel diameters throughout the flow route, due to the increased confining force. The estimated value of exponent C is higher (2.8) for specimen S1-04 than other specimens, which accounts for the higher capillary number. No direct relationship between the parameter and capillary number is established is this study. The experimental data as well as the mathematical model's prediction for immiscible two-phase flow through wellbore cement fracture is plotted in Figure 3.9.

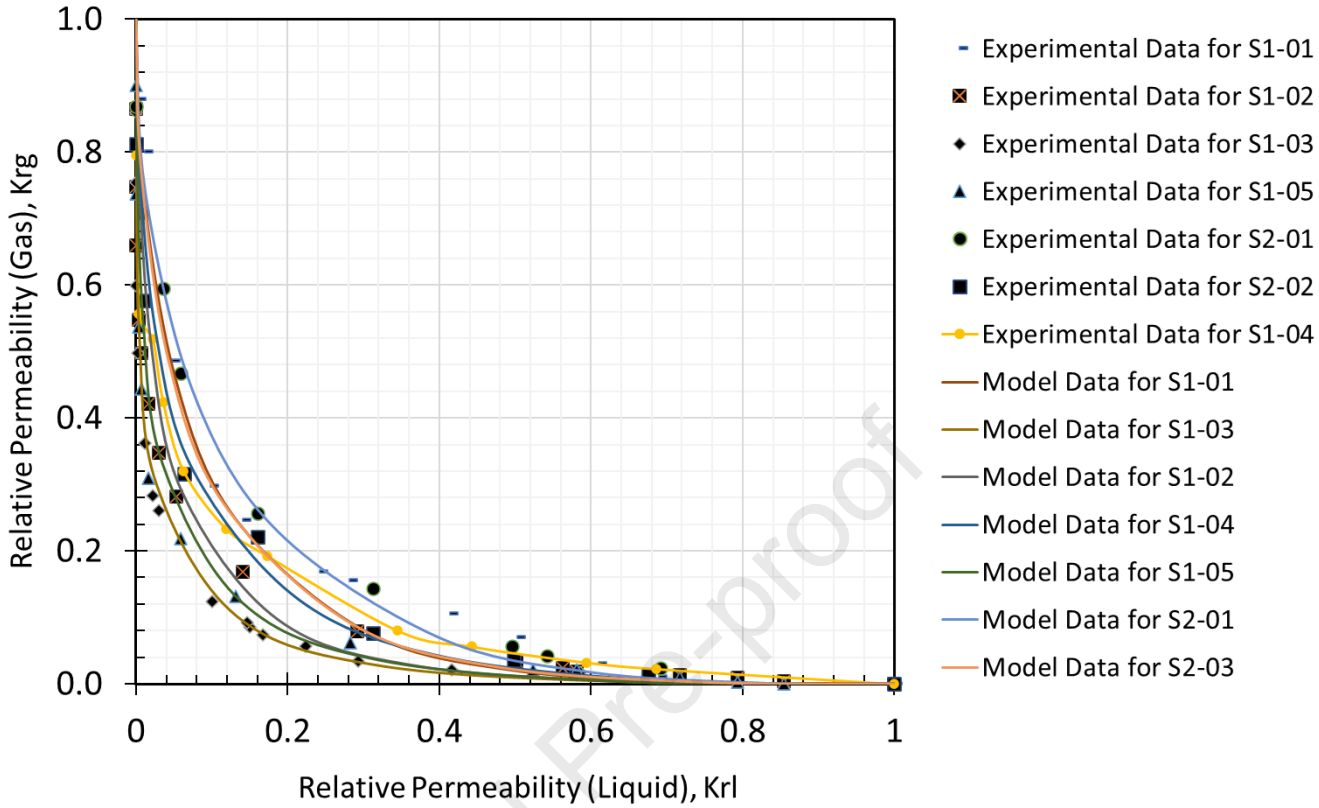

Figure 3.9 - The experimental data and mathematical model prediction for immiscible two-phase flow through a wellbore cement fracture, with $R^2 > 0.84$.

As presented in Figure 3.9, relative permeability measurements for each specimen are compared with the associate model, made for each saturation. Using Student t-statistics, it was observed that the obtained P-values are more than 0.05 for each pair of observed and predicted data set. The obtained P-values were substantially high (> 9.5). These results suggest that at 0.05 level of significance, the model's prediction and the experimentally obtained data are the same.

The proposed mathematical model for two-phase flow can be helpful in accounting for the complex interactions between different fluids phase present in a leaky wellbore. With further validation of the model, our study presents a major step forward towards the realistic simulation of leakage dynamics for two-phase flow through the leaky wellbores. The insights gained from understanding flow behavior through the proposed two-phase model are invaluable for optimizing remediation and intervention efforts. Additionally, the

two-phase flow model may help in fulfilling the requirements for comprehensive analysis necessary for safety and risk assessments, as well as for regulatory compliance and reporting.

4. Conclusion

Relative permeabilities of the simultaneous two-phase flow through fractured cement specimen are measured for different confining stresses, viscosity ratios and capillary numbers. The results reveal that, in addition to flow saturation, the two-phase flow relative permeability depends on the flow path tortuosity, aperture size, viscosity ratio, and capillary number. We have also observed that, for wellbore cement fractures, the sum of the wetting and non-wetting phase relative permeabilities is smaller than one, which indicates that strong phase interference exists. Therefore, the X-model for two-phase flow is not useful for oil-well cement fractures filled with fluids of multiple phases.

The fracture aperture is mainly controlled by confining stress, which substantially affects two-phase flow behavior. The change in confining stress not only alters the amount of fluid flow but also changes the contact area and the flow path tortuosity. The pressure-sensitive films from the specimen fractures at two different confining stresses are analyzed to evaluate the change in contact area due to the increment in confining stress. The roughness coefficients before and after the flow test is also reported that affects the transition from linear to nonlinear flow. The study shows that at comparatively higher confining stress (13.8 MPa; 2000 psig), the fracture network can be modeled as a porous media, and the viscous coupling effect is negligible.

The relative permeability of the non-wetting phase also varies with the viscosity ratio. At the highest oil saturation, the effect of the viscosity ratio is negligible. The measured two-phase relative permeabilities could not be fully described by either the viscous coupling model or Corey's model.

The relative permeability of the non-wetting phase also varies with the flow capillary number. The relative permeabilities for the fracture with the lower capillary number cannot be fully modeled using either the viscous coupling or Corey's model. The results suggests

that, for higher Ca shows that at higher to intermediate saturation, the viscous coupling model may reasonably estimate the permeability of the individual phases. None of the commonly used models can completely describe the relative permeabilities of individual phases for the different capillary number.

All test results are corrected for slippage effect and non-linear (i.e., visco-inertial) flow as necessary and interpreted in terms of either relative permeability (two-phase flow) or hydraulic apertures (single-phase flow) of the fractures. Both the gas slip factor and the coefficient of inertial resistance for all flow test measurements are reported and empirical relationships are presented to easily correct the leakage data that will be beneficial for field application.

The current study presents a mathematical model capable of describing the relationship between relative permeabilities for two-phase flow through wellbore cement fractures. The statistical analysis demonstrates that the model's prediction and the data collected through experimentation are comparable. The difference between the model results and the experimental data obtained in this study are negligible. The exact value of the required parameters in the mentioned mathematical model may vary for certain fluids. This model must be further examined with available data on pertinent caverns fluid, and then it can be useful for calculating the overall leakage from a leaky wellbore's well head monitoring system.

In order to directly apply the roughness and confining stress data collected in this study to the aforementioned mathematical model, future research may involve extensive computer modeling.

Acknowledgement

The experimental study is a part of the Strategic Petroleum Reserve (SPR) wellbore flow project and is funded by Sandia National Laboratories. Sandia National Laboratories is a multi-mission laboratory managed and operated by National Technology & Engineering Solutions of Sandia, LLC, a wholly owned subsidiary of Honeywell International Inc., for the U.S. Department of Energy’s National Nuclear Security Administration under contract

DE-NA0003525. This research describes objective technical results and future research plans. Any subjective views or opinions that might be expressed in the document do not necessarily represent the views of the U.S. Department of Energy or the United States Government. LA-UR 23-28715.

References

Ansari, A. M., Sylvester, N. D., Shoham, O., & Brill, J. P. (1990). A comprehensive mechanistic model for upward two-phase flow in wellbores. *SPE Annual Technical Conference and Exhibition*. Society of Petroleum Engineers.

Anwar, I., Carey, B., Johnson, P., & Donahue, C. (2022). Detecting and characterizing fluid leakage through wellbore flaws using Fiber-Optic Distributed Acoustic Sensing. *ARMA US Rock Mechanics/Geomechanics Symposium*, ARMA-2022. ARMA.

Anwar, I., Carey, J. W., Johnson, P. A., & Donahue, C. (2021). Evaluating Two-Phase Flow through Wellbore Cement Fractures using Fiber-Optic Distributed Acoustic Sensing. *AGU Fall Meeting 2021*. AGU.

Anwar, I., Chojnicki, K., Bettin, G., Taha, M. R., & Stormont, J. C. (2019). Characterization of wellbore casing corrosion product as a permeable porous medium. *Journal of Petroleum Science and Engineering*, *180*, 982–993.

Anwar, I., Hatambeigi, M., Chojnicki, K., Reda Taha, M., & Stormont, J. (2020). *Relative permeabilities for two-phase flow through wellbore cement fractures.* Sandia National Lab.(SNL-NM), Albuquerque, NM (United States).

Anwar, I., Hatambeigi, M., & Stormont, J. (2019). *Profiler: An autonomous instrument for scanning and determining the material surface roughness*. US: Provisional Pat. Ser. No. 62/885,711.

Babadagli, T, Raza, S., Ren, X., & Develi, K. (2015). Effect of surface roughness and lithology on the water–gas and water–oil relative permeability ratios of oil-wet single fractures. *International Journal of Multiphase Flow*, *75*, 68–81.

Babadagli, Tayfun, Ren, X., & Develi, K. (2015). Effects of fractal surface roughness and

lithology on single and multiphase flow in a single fracture: an experimental investigation. *International Journal of Multiphase Flow*, *68*, 40–58.

Bandis, S. C., Lumsden, A. C., & Barton, N. R. (1983). Fundamentals of rock joint deformation. *International Journal of Rock Mechanics and Mining Sciences & Geomechanics Abstracts*, *20*(6), 249–268. Elsevier.

Barelli, A., Corsi, R., Del Pizzo, G., & Scali, C. (1982). A two-phase flow model for geothermal wells in the presence of non-condensable gas. *Geothermics*, *11*(3), 175–191.

Bear, J. (1972). Dynamics of flow in porous media. In *American Elsevier* (p. 764).

Berkowitz, B. (2002). Characterizing flow and transport in fractured geological media: A review. *Advances in Water Resources*, *25*(8–12), 861–884.

Bhushan, B. (2001). Tribology on the macroscale to nanoscale of microelectromechanical system materials: a review. *Proceedings of the Institution of Mechanical Engineers, Part J: Journal of Engineering Tribology*, *215*(1), 1–18.

Brooks, R., & Corey, T. (1964). HYDRAU uc properties of porous media. *Hydrology Papers, Colorado State University*, *24*, 37.

Burdine, N. (1953). Relative permeability calculations from pore size distribution data. *Journal of Petroleum Technology*, *5*(03), 71–78.

Celia, M. A., Bachu, S., Nordbotten, J. M., Gasda, S. E., & Dahle, H. K. (2005). - Quantitative estimation of CO 2 leakage from geological storage: Analytical models, numerical models, and data needs. In *Greenhouse Gas Control Technologies 7* (pp. 663–671). Elsevier.

Chen, C., & Horne, R. N. (2006). Two-phase flow in rough-walled fractures: Experiments and a flow structure model. *Water Resources Research*, *42*(3).

Chen, Y.-F., Wu, D.-S., Fang, S., & Hu, R. (2018). Experimental study on two-phase flow in rough fracture: Phase diagram and localized flow channel. *International Journal of Heat and Mass Transfer*, *122*, 1298–1307.

Chen, Y.-F., Zhou, J.-Q., Hu, S.-H., Hu, R., & Zhou, C.-B. (2015). Evaluation of Forchheimer equation coefficients for non-Darcy flow in deformable rough-walled fractures. *Journal of Hydrology*, *529*, 993–1006.

Cooke Jr, C. E. (1973). Conductivity of fracture proppants in multiple layers. *Journal of Petroleum Technology*, *25*(09), 1101–1107.

Corey, A. T. (1954). The interrelation between gas and oil relative permeabilities. *Producers Monthly*, *19*(1), 38–41.

Davies, R. J., Almond, S., Ward, R. S., Jackson, R. B., Adams, C., Worrall, F., … Whitehead, M. A. (2014). Oil and gas wells and their integrity: Implications for shale and unconventional resource exploitation. *Marine and Petroleum Geology*, *56*, 239–254. https://doi.org/https://doi.org/10.1016/j.marpetgeo.2014.03.001

De Gennes, P. G. (1983). Hydrodynamic dispersion in unsaturated porous media. *Journal of Fluid Mechanics*, *136*, 189–200.

Diomampo, G. (2001). *Relative permeability through fractures*. Stanford University, Stanford, CA.

Dranchuk, P. M., & Kolada, L. J. (1968). Interpretation of steady linear visco-inertial gas flow data. *Journal of Canadian Petroleum Technology*, *7*(01), 36–40.

Duncan, N., & Hancock, K. E. (1966). The concept of contact stress in the assessment of the behaviour of rock masses as structural foundations. *1st ISRM Congress*. OnePetro.

Fairhurst, C. (1964). On the validity of the 'Brazilian'test for brittle materials. *International Journal of Rock Mechanics and Mining Sciences & Geomechanics Abstracts*, *1*(4), 535–546. Elsevier.

Farrell, D. A., & Larson, W. E. (1972). Modeling the pore structure of porous media. *Water Resources Research*, *8*(3), 699–706.

Forchheimer, P. (1901). Wasserbewegung durch Boden. *Z. Ver. Deutsch. Ing*, (45), 1782–1788.

Fourar, M., & Bories, S. (1995). Experimental study of air-water two-phase flow through a fracture (narrow channel). *International Journal of Multiphase Flow*, *21*(4), 621–637.

Fourar, M., Bories, S., Lenormand, R., & Persoff, P. (1993). Two-phase flow in smooth and rough fractures: Measurement and correlation by porous-medium and pipe flow models. *Water Resources Research*, *29*(11), 3699–3708.

Fourar, M., Piquemal, J., & Bories, S. (1991). Ecoulement diphasique bidimensionnel plan liquid-gaz. II, Gradients de pression et fractions volumiques des phases d'un écoulement horizontal. *Comptes Rendus de l'Académie Des Sciences. Série 2, Mécanique, Physique, Chimie, Sciences de l'univers, Sciences de La Terre*, *313*(5), 477–480.

Gardner, W. R. (1958). Some steady-state solutions of the unsaturated moisture flow equation with application to evaporation from a water table. *Soil Science*, *85*(4), 228–232.

Geertsma, J. (1974). Estimating the coefficient of inertial resistance in fluid flow through porous media. *Society of Petroleum Engineers Journal*, *14*(05), 445–450.

Gomez, L. E., Shoham, O., Schmidt, Z., Chokshi, R. N., & Northug, T. (2000). Unified mechanistic model for steady-state two-phase flow: horizontal to vertical upward flow. *SPE Journal*, *5*(03), 339–350.

Gould, T. L. (1974). Vertical two-phase steam-water flow in geothermal wells. *Journal of Petroleum Technology*, *26*(08), 833–842.

Guerrero, C., Reyes, E., & González, V. (2002). Fracture surface of plastic materials: the roughness exponent. *Polymer*, *43*(25), 6683–6693.

He, S., Kahanda, G. L., & Wong, P. (1992). Roughness of wetting fluid invasion fronts in porous media. *Physical Review Letters*, *69*(26), 3731.

Heid, J. G., McMahon, J. J., Nielsen, R. F., & Yuster, S. T. (1950). Study of the

permeability of rocks to homogeneous fluids. *Drilling and Production Practice*. American Petroleum Institute.

Heller, R., Vermylen, J., & Zoback, M. (2014a). Experimental investigation of matrix permeability of gas shales. *AAPG Bulletin*, *98*(5), 975–995.

Heller, R., Vermylen, J., & Zoback, M. (2014b). Experimental investigation of matrix permeability of gas shalesExperimental Investigation of Matrix Permeability of Gas Shales. *AAPG Bulletin*, *98*(5), 975–995.

Ho, C. K., & Webb, S. W. (2006). *Gas transport in porous media* (Vol. 20). Springer.

Holtzman, R. (2016). Effects of pore-scale disorder on fluid displacement in partially-wettable porous media. *Scientific Reports*, *6*, 36221.

Holtzman, R., & Juanes, R. (2010). Crossover from fingering to fracturing in deformable disordered media. *Physical Review E*, *82*(4), 46305.

Holtzman, R., & Segre, E. (2015). Wettability stabilizes fluid invasion into porous media via nonlocal, cooperative pore filling. *Physical Review Letters*, *115*(16), 164501.

Iwai, K. (1976). Fundamentals of fluid flow through a single fracture. *Ph. D. Thesis*. University of California Berkeley.

Jones, F. O., & Owens, W. W. (1980). A laboratory study of low-permeability gas sands. *Journal of Petroleum Technology*, *32*(09), 1–631.

Joshi, N. B., Mullins, O. C., Jamaluddin, A., Creek, J., & McFadden, J. (2001). Asphaltene precipitation from live crude oil. *Energy & Fuels*, *15*(4), 979–986.

Kalaydjian, F., & Legait, B. (1987). Perméabilités relatives couplées dans des écoulements en capillaire et en milieu poreux. *Comptes Rendus de l'Académie Des Sciences. Série 2, Mécanique, Physique, Chimie, Sciences de l'univers, Sciences de La Terre*, *304*(17), 1035–1038.

Karpyn, Z. T., Grader, A. S., & Halleck, P. M. (2007). Visualization of fluid occupancy in a rough fracture using micro-tomography. *Journal of Colloid and Interface Science*, *307*(1), 181–187.

Kaya, A. S., Sarica, C., & Brill, J. P. (2001). Mechanistic modeling of two-phase flow in deviated wells. *SPE Production & Facilities*, *16*(03), 156–165.

Klinkenberg, L. J. (1941). The permeability of porous media to liquids and gases. *Drilling and Production Practice*. American Petroleum Institute.

Kouame, S. K. (1989). *Étude expérimentale d'écoulements diphasiques en fracture*. Toulouse, INPT.

Kundu, P. K., Cohen, I. M., & Dowling, D. (2008). *Fluid Mechanics 4th*. Elsevier.

Lenormand, R., Touboul, E., & Zarcone, C. (1988). Numerical models and experiments on immiscible displacements in porous media. *Journal of Fluid Mechanics*, *189*, 165–187.

Lenormand, R., Zarcone, C., & Sarr, A. (1983). Mechanisms of the displacement of one fluid by another in a network of capillary ducts. *J. Fluid Mech*, *135*(34), 337–353.

Lockhart, R. W., & Martinelli, R. C. (1949). Proposed correlation of data for isothermal two-phase, two-component flow in pipes. *Chem. Eng. Prog*, *45*(1), 39–48.

Maloney, D., & Doggett, K. (1997). Multiphase Flow in Fractures. *International Symposium of the Society of Core Analysts*, p. 11. Retrieved from http://www.ux.uis.no/~s-skj/ipt/Proceedings/SCA.1987-2004/1-SCA1997-30.pdf

McCain Jr, W. D. (2017). *Properties of petroleum fluids*. PennWell Corporation.

Miyazaki, B. (2009). Well integrity: An overlooked source of risk and liability for underground natural gas storage. Lessons learned from incidents in the USA. *Geological Society, London, Special Publications*, *313*(1), 163–172.

Mualem, Y. (1976). A new model for predicting the hydraulic conductivity of unsaturated porous media. *Water Resources Research*, *12*(3), 513–522.

Mullins, O. C. (2008). *physics of reservoir fluids*. Schlumberger.

Nemer, M. B., Kuhlman, K. L., Newell, P., & Bettin, G. (2016). *Strategic Petroleum Reserve Cemented Annulus Modeling and Testing; FY16 Progress.* Sandia National Lab.(SNL-NM), Albuquerque, NM (United States).

Nicholl, M. J., & Glass, R. J. (2005). Infiltration into an analog fracture: Experimental observations of gravity-driven fingering. *Vadose Zone Journal*, *4*(4), 1123–1151.

Nowamooz, A., Radilla, G., & Fourar, M. (2009). Non-Darcian two-phase flow in a transparent replica of a rough-walled rock fracture. *Water Resources Research*, *45*(7). https://doi.org/10.1029/2008WR007315

Or, D. (2008). Scaling of capillary, gravity and viscous forces affecting flow morphology in unsaturated porous media. *Advances in Water Resources*, *31*(9), 1129–1136.

Ortiz, L., Volckaert, G., & Mallants, D. (2002). Gas generation and migration in Boom Clay, a potential host rock formation for nuclear waste storage. *Engineering Geology*, *64*(2–3), 287–296.

Persoff, P. G., & Pruess, K. (1993). *Flow visualization and relative permeability measurements in rough-walled fractures*.

Persoff, P. G., Pruess, K., & Myer, L. (1991). *Two-phase flow visualization and relative permeability measurement in transparent replicas of rough-walled rock fractures*.

Persoff, P., & Pruess, K. (1995). Two-phase flow visualization and relative permeability measurement in natural rough-walled rock fractures. *Water Resources Research*, *31*(5), 1175–1186.

Pirson, S. J. (1958). Oil Reservoir Engineering, Mc-G. raw-Hill Book Co. *Inc., NY*.

Postgate, J. R. (1979). *The sulphate-reducing bacteria*. CUP Archive.

Pruess, K., & Tsang, Y. W. (1990). On two-phase relative permeability and capillary pressure of rough-walled rock fractures. *Water Resources Research*, *26*(9), 1915–1926.

Qiao, Y., Skadsem, H. J., & Evje, S. (2023). An Integrated Modeling Approach for Vertical Gas Migration Along Leaking Wells Using a Compressible Two-Fluid Flow Model.

Transport in Porous Media, *150*(1), 177–213.

Radilla, G., Nowamooz, A., & Fourar, M. (2013). Modeling non-Darcian single-and two-phase flow in transparent replicas of rough-walled rock fractures. *Transport in Porous Media*, *98*(2), 401–426.

Raven, K. G., & Gale, J. E. (1985). Water flow in a natural rock fracture as a function of stress and sample size. *International Journal of Rock Mechanics and Mining Sciences & Geomechanics Abstracts*, *22*(4), 251–261. Elsevier.

Reardon, E. J. (1995). Anaerobic corrosion of granular iron: Measurement and interpretation of hydrogen evolution rates. *Environmental Science & Technology*, *29*(12), 2936–2945.

Reinecke, S. A., & Sleep, B. E. (2002). Knudsen diffusion, gas permeability, and water content in an unconsolidated porous medium. *Water Resources Research*, *38*(12).

Reitsma, S., & Kueper, B. H. (1994). Laboratory measurement of capillary pressure-saturation relationships in a rock fracture. *Water Resources Research*, *30*(4), 865–878.

Ren, F., Ma, G., Wang, Y., Fan, L., & Zhu, H. (2017). Two-phase flow pipe network method for simulation of CO2 sequestration in fractured saline aquifers. *International Journal of Rock Mechanics and Mining Sciences*, *98*, 39–53.

Reynolds, D A, & Kueper, B. H. (2002). Numerical examination of the factors controlling DNAPL migration through a single fracture. *Groundwater*, *40*(4), 368–377.

Reynolds, David A, & Kueper, B. H. (2001). Multiphase flow and transport in fractured clay/sand sequences. *Journal of Contaminant Hydrology*, *51*(1–2), 41–62.

Romm, E. S. (1966). Flow characteristics of fractured rocks. *Nedra, Moscow*, *283*.

Rushing, J. A., Newsham, K. E., Lasswell, P. M., Cox, J. C., & Blasingame, T. A. (2004). Klinkenerg-corrected permeability measurements in tight gas sands: steady-state versus unsteady-state techniques. *SPE Annual Technical Conference and Exhibition*. Society of Petroleum Engineers.

Ruth, D., & Ma, H. (1992). On the derivation of the Forchheimer equation by means of the averaging theorem. *Transport in Porous Media*, *7*(3), 255–264.

Saffman, P. G., & Taylor, G. I. (1958). The penetration of a fluid into a porous medium or Hele-Shaw cell containing a more viscous liquid. *Proceedings of the Royal Society of London. Series A. Mathematical and Physical Sciences*, *245*(1242), 312–329.

Shadravan, A., Ghasemi, M., & Alfi, M. (2015). Zonal isolation in geothermal wells. *Proceedings, Fortieth Workshop on Geothermal Reservoir Engineering Stanford University*, 1–10.

Shaibu, R., Sambo, C., Guo, B., & Dudun, A. (2021). Advances in Geo-Energy Research. *Ager*, 7.

Tiss, M., & Evans, R. D. (1989). Measurement and correlation of non-Darcy flow coefficient in consolidated porous media. *Journal of Petroleum Science and Engineering*, *3*(1–2), 19–33.

Toner, G. (1987). The International Energy Agency and the development of the stocks decision. *Energy Policy*, *15*(1), 40–58.

Van Genuchten, M. T. (1980). A closed-form equation for predicting the hydraulic conductivity of unsaturated soils 1. *Soil Science Society of America Journal*, *44*(5), 892–898.

Wang, M., Chen, Y.-F., Ma, G.-W., Zhou, J.-Q., & Zhou, C.-B. (2016). Influence of surface roughness on nonlinear flow behaviors in 3D self-affine rough fractures: Lattice Boltzmann simulations. *Advances in Water Resources*, *96*, 373–388.

Watson, Theresa L, & Bachu, S. (2009). Evaluation of the potential for gas and CO2 leakage along wellbores. *SPE Drilling & Completion*, *24*(01), 115–126.

Watson, Theresa Lucy, & Bachu, S. (2008). Identification of wells with high CO2-leakage potential in mature oil fields developed for CO2-enhanced oil recovery. *SPE Symposium on Improved Oil Recovery*. Society of Petroleum Engineers.

Witherspoon, P. A., Wang, J. S. Y., Iwai, K., & Gale, J. E. (1980). Validity of Cubic Law for fluid flow in a deformable rock fracture. *Water Resources Research*, *16*(6), 1016–1024. https://doi.org/10.1029/WR016i006p01016

Wong, R., Pan, X., & Maini, B. B. (2008). Correlation between pressure gradient and phase saturation for oil-water flow in smooth-and rough-walled parallel-plate models. *Water Resources Research*, *44*(2).

Zeng, Z., & Grigg, R. (2006). A Criterion for Non-Darcy Flow in Porous Media. *Transport in Porous Media*, *63*(1), 57–69. https://doi.org/10.1007/s11242-005-2720-3

Zhang, C., Oostrom, M., Wietsma, T. W., Grate, J. W., & Warner, M. G. (2011). Influence of viscous and capillary forces on immiscible fluid displacement: Pore-scale experimental study in a water-wet micromodel demonstrating viscous and capillary fingering. *Energy & Fuels*, *25*(8), 3493–3505.

Zhang, M., & Bachu, S. (2011). Review of integrity of existing wells in relation to CO2 geological storage: What do we know? *International Journal of Greenhouse Gas Control*, *5*(4), 826–840.

Zhang, Z., & Nemcik, J. (2013). Fluid flow regimes and nonlinear flow characteristics in deformable rock fractures. *Journal of Hydrology*, *477*, 139–151.

Zhou, J.-Q., Hu, S.-H., Fang, S., Chen, Y.-F., & Zhou, C.-B. (2015). Nonlinear flow behavior at low Reynolds numbers through rough-walled fractures subjected to normal compressive loading. *International Journal of Rock Mechanics and Mining Sciences*, *80*, 202–218.

Zimmerman, R. W., Al-Yaarubi, A., Pain, C. C., & Grattoni, C. A. (2004). Non-linear regimes of fluid flow in rock fractures. *International Journal of Rock Mechanics and Mining Sciences*, *41*, 163–169.

Declarations

Author Contributions

Dr. Ishtiaque Anwar contributed to the conceptualization, methodology design, conducting experimental research, formal analysis, and data collection. He was also responsible for preparing the manuscript's first draft and was heavily involved in the writing, reviewing, and editing procedures, as well as finishing it. Dr. Mahya Hatambeigi provided assistance in the experimental data collection. Dr. David L. Lord and David B. Hart both contributed to reviewing and editing the manuscript, as well as securing funding for the research. Dr. Mahmoud Reda Taha was involved in validating the research findings and contributed to the writing, reviewing, and editing stages of the manuscript. Dr. Meng Meng was engaged in the review of the manuscript. Dr. John C. Stormont provided general supervision to conceptualize the study's approach, writing, reviewing, and editing the manuscript.

Competing Interest

The authors have no relevant financial or non-financial interests to disclose.

Data Availability

The datasets generated during and/or analyzed during the current study are available from the corresponding author on reasonable request.

Highlights:

- Commonly used models for two-phase models are not always capable of accurately predicting the relative permeabilities for wellbore cement fracture.
- For two-phase flow through wellbore cement fracture or comparatively smaller aperture exhibits significant phase interference.
- Relative permeability is intricately influenced by saturation, flow path tortuosity, aperture size, viscosity ratio, and flow capillary number.
- A new mathematical model for estimating the relative permeability of wellbore cement fracture is presented and validated.

Declaration of interests

☐ The authors declare that they have no known competing financial interests or personal relationships that could have appeared to influence the work reported in this paper.

☒ The authors declare the following financial interests/personal relationships which may be considered as potential competing interests:

John C. Stormont reports financial support was provided by Sandia National Laboratories. If there are other authors, they declare that they have no known competing financial interests or personal relationships that could have appeared to influence the work reported in this paper.